Optimal control in a micro grid of households equipped with μ-CHPs and energy storage devices

Julia Botella
s2814889

Supervised by:
Prof. Dr. Ir. Jacquelien M. A. Scherpen
Prof. Dr. Ming Cao
Desti Alkano, MSc

FACULTY OF MATHEMATICS AND NATURAL SCIENCES

Discrete Technology & Production Automation (DTPA) Research Group

Optimal control in a micro grid of households equipped with μ-CHPs and energy storage devices

J. Botella

September 15, 2015

Abstract

This work studies optimal flow control of a micro grid consisting of households equipped with μ-CHP devices and gas and heat buffers. Agricultural wastes from households are used to produce biogas by a biogas generator. The produced biogas is, then, utilized to fulfill local demand of heat and power of the households. Excess biogas can be upgraded and sold to the low pressure gas grid. Excess electricity produced by the μ-CHPs of households can be also sold to the electricity grid. The aim of the control process is to maximize the estimated profit of the households while avoiding overloading gas and electricity grids and avoiding the biogas shortage. The decisions on the supply and consumption levels are done in both centralized and distributed fashions using model predictive control (MPC). The distributed MPC (dMPC) is developed from the centralized MPC (cMPC) by employing dual decomposition method combined with the projected sub-gradient method. In dMPC, each household makes decisions based on its local information, yet still needs to coordinate its supply and consumption bids to the grid operators and the biogas generator. The coordinations are formulated for synchronous and asynchronous implementations. With the distributed scheme, the grid operators and the biogas producer can manage households' supply and consumption levels via dynamic pricing to obey the grid capacity constraints. We perform extensive simulations to investigate the behavior of dynamic pricing modified by the grid operators and the biogas generator. Furthermore, we provide numerical results to compare the performance of cMPC, synchronous dMPC, and asynchronous dMPC using realistic estimates of the selling prices and demand patterns.

Contents

List of Figures

List of Tables

Chapter 1

Introduction

This chapter will introduce the topic of this research project. The motivation of the research is explained firstly, followed by research focus and research background. Finally, the thesis outline is given.

1.1 Research motivation

Due to the worldwide environmental problems related to energy usage and depletion of fossil resources, there is need for a more sustainable energy system, as well as using cleaner energy resources. In order to reduce the needs of electricity, distributed power generation in the future smart grid gives a key to optimize the efficiency of the energy chain. Its main advantage is that, when the produced power is used in the local neighborhood (i.e. as close as possible to the production point), transmission losses in the power network are avoided.

So as to improve global efficiency and use cleaner resources, cogeneration or Combined Heat and Power production (known as *CHP*) is also pointed out as a promising investment, since it offers several advantages over the conventional heat production such as a higher global efficiency and high-quality electricity, among others. Moreover, it can be fuelled on biogas [1], which can be obtained from biomass. Therefore, using CHP devices, it is possible to get energy and heat in an efficient manner while also reusing wastes.

A micro-scale CHP device, useful for meeting residential demands, is known as μ-CHP. In the context of the EU 2020 objectives, micro-CHP (micro-scale CHP) systems can contribute to a reduction of CO_2 emissions in both the residential and commercial sectors and to an increase of the energy performance (efficiency) of existing buildings. Typically, μ-CHP are also run on gas, which makes them particularly interesting to install in households in countries like the Netherlands where the gas grid is dense [2]. From a business point of view, their potential is considered to be high, see for example [3] or [4].

In fact, in the north of the Netherlands a demonstration project of a future smart grid (with 25 households in the first phase and 42 in the second phase) called Power-Matching city was implemented and its results demonstrated that smart energy systems are technically feasible and that energy flexibility makes economic sense. The net gains from the consumer market could well reach 3.5 billion euros [5].

1.2 Research focus

Commonly, studies on control systems for implementations with μ-CHP technologies often add an auxiliary burner and heat storage device to the μ-CHP's prime mover, see e.g. [6] or [7]. In this work we aim to design a control mechanism for a setup similar to the one in [8] adding a gas storage device and using, instead of natural gas, biogas produced in an anaerobic digester in the neighborhood [1], [9].

Therefore, the focus of the research will be implementing a control mechanism for a micro-grid consisting of a community of households producing agricultural wastes, and using an anaerobic digester to turn these wastes into biogas. With the biogas, each household will be able to produce heat and power energy using the μ-CHP and fulfill its own local heat and power demand. Each household will be connected to the electricity grid and to the shared biogas upgrader, connected to the low pressure gas grid.

The desired control system is a distributed control mechanism which is able to optimize the supply and consumption plan for every household of the community.

1.3 Recent work

In [10] two different methods to control a small network of μ-CHP's are compared: the Power-Matcher method [11] (proposed in a centralized fashion) and a decentralized control structure where households make individual decisions taking into account only their own circumstances. Both control methods are compared based on the total costs of the system, the total amount of resources required and the peak load reduction. Results are obtained by a simulation study in which the control methods were tested on a network of five households. The main conclusions of the research were that the fuel cell generator combined with the PowerMatcher method is the best option, since the simulations result in lower total costs of the system and less resources required [10]. However, the fuel cell generator was not yet commercially available due to major issues regarding reliability and safety. Nowadays it is commercially available and the country which is leading its commercialization and development is Japan [14]. In general it is concluded that the principles of the PowerMatcher method work, but with some major problems. Also, other forms of electricity generation should be taken into account, as the lack of heat demand in the summer restricts the usage of the μ-CHP [10].

In [16] and [12], the authors exposed a new mechanism to control the network of μ-CHPs. Such control mechanism is based on a control strategy like the one presented in [13]. In [13], Rantzer combines Linear Quadratic control theory with dynamic dual decomposition. In this work, it is shown that dual decomposition helps to convert a team problem (e.g. reducing electricity imbalance) into a non-cooperative problem, where each player has its own goal. When each player optimizes its own objective function, the common objective function will be optimized as well. The main point of dynamic dual decomposition is the introduction of Lagrange multipliers between the players, which can be interpreted as price signals the players pay each other. In order to achieve the optimal value of the objective function, each player aims to reduce his/her costs. In the first method [13], only one equilibrium electricity market price over the whole network exists while in Rantzer's method different prices are considered, one for every pair of households, represented by the Lagrangian multiplers [12].

In [8], Larsen et al. showed that the network of μ-CHPs can be modelled with an alternative control mechanism, which enables to add constraints to the cost function. As in [13], dynamic dual decomposition is used to convert the team problem to a non-cooperative problem by the introduction of Lagrange multipliers. Instead of Linear Quadratic Control the optimization is performed with Model Predictive Control [17], as it is able to handle constraints in the cost function.

1.4 Research goal

The goal of the work is to apply Model Predictive Control on the use of biogas fuelled μ-CHP owned by a prosumer with the aim of achieving the economically optimal supply and consumption plan while complying all the technical constraints.

Two approaches to the problem will be presented and solved. First, it will be assumed that there is a **central controller**, who receives all the information from the grids, biogas producer, and from the prosumers. This central controller will be the one optimizing the production level for each prosumer i. The second approach will be a **distributed** one. However, as explained later in Section 3.2.4, it is not possible to achieve a fully distributed model in this case. Therefore, in this distributed approach it will be assumed that there is an exchange of information between the prosumers and the operators of the grids and the biogas producer, allowing each prosumer to solve its own optimization problem with given information.

The main question that this thesis aims to answer is: *What is a possible algorithm to economically optimize the energy consumption and production of a micro-grid of households equipped with μ-CHP and energy buffers?*

The following subquestions are derived from the main question.

- How can a typical setup of a community of households be?
- How can a household equipped with μ-CHP and heat and biogas storage devices

be modeled, aiming to satisfy its local demand and interact with the power and low pressure gas grids?

- What are the requirements for the control mechanism?
- What is the most appropriate control mechanism?
- How can the problem be solved in a centralized manner and in a distributed fashion?
- What happens if the operator of one grid does not have access to the same clock that prosumers use?
- How do Lagrangian multipliers behave in dMPC implementation?

1.5 Thesis outline

To answer the research question this thesis is organized as follows:

- In Chapter 2 the model representing a micro-grid of households equipped with μ-CHPs and energy buffers is constructed. This is done by a description of each member. In this chapter, a brief explanation of the technical devices interacting in or with the studied system is given.
- In Chapter 3, we develop two different control schemes based on model predictive control (MPC). The general concept of MPC is discussed here after it is applied to our network model. This will first result in a centralized controller. Dual decomposition is used to reformulate the centralized control to obtain a distributed control scheme.
- In Chapter 4, we investigate the performance of the formulated controllers by means of simulations. Simulations performed are described in detail and performance indicators are formulated to compare different control mechanisms. We focus in the distributed simulations in how the Lagrangian multipliers behave.
- In Chapter 5, some discussion is performed and some conclusions are drawn.

Chapter 2

Model of a micro grid connected to external energy grids

In this chapter, the micro-grid is explained first, and all the agents participating in or with the grid are explained later.

The micro grid studied in this work consists of a group of nearby households equipped with μ-CHPs and energy storage devices. The micro grid, or community, is illustrated in Figure 2.1. The goal of the micro grid is to share the costs of some facilities that allow them to produce and utilize energy in an efficient manner. The first shared facility is an anaerobic digester, used to generate biogas from agriculture wastes collected by the households. The produced biogas can be, then, used to generate power and heat by using μ-CHP devices. From now on, the owner of a household is called *prosumer* as it also consumes the produced energy. The second facility that prosumers share is a gas upgrader, which receives the produced biogas that prosumers want to upgrade to green gas before selling it to the low pressure gas grid.

2.1 Facilities shared by the micro grid

As mentioned before, the community share two main facilities. These facilities are explained deeper in this section.

2.1.1 Biogas producer

The biomass obtained from agriculture wastes in the households can be converted into biogas in an anaerobic digester.

Anaerobic digestion of organic wastes and by-products from agriculture and the food industry is a process known for many years and is widely used for waste stabilization, pollution control, improvement of manure quality and biogas production. It is

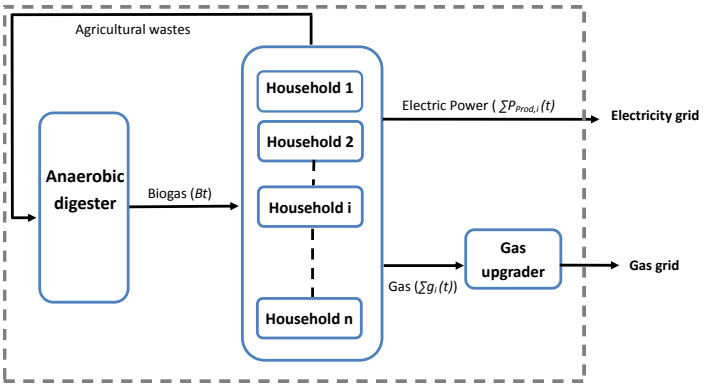

Figure 2.1: Scheme of a community of households equipped with μ-CHP and energy storage devices, modified from [15]

.

a technology which demonstrates many advantages. It can convert a disposal problem into a profit center, it allows agricultural crops to be converted into a highly valuable fuel and it can replace mineral fertilization by nutrient recovery. Therefore, anaerobic digestion has become a key method for both waste treatment and the production of renewable fuels [30].

The anaerobic digestion is a naturally occurring biological process in which organic material is broken down by bacteria in a low-oxygen environment resulting in the generation of methane gas and carbon dioxide as its two primary products. An anaerobic digester is, by definition, a device for optimizing the anaerobic digestion of biomass and/or animal manure, often used to recover biogas for energy production. Commercial digester types include complete mix, continuous flow (horizontal or vertical plug-flow, multiple-tank, and single tank) and covered lagoon [32].

Anaerobic digester systems have been used for decades at municipal waste-water facilities, and more recently, have been used to process industrial and agricultural wastes [29]. These systems are designed to optimize the growth of the methane-forming bacteria that generate CH_4. Typically, using organic wastes as the major input, the systems produce biogas that contains 55% to 70% CH_4 and 30% to 40% CO_2 [32].

It is chosen to be a shared facility since the cost of the production of an anaerobic digester decreases with bigger capacities (scalable costs) and most of the anaerobic

digesters need a minimum amount of organic waste to use, hardly achievable by a single household [32] [30].

2.1.2 Biogas Upgrader

If there is some gas that prosumers don't want to use nor store, they can sell it to the low pressure gas grid. For doing so, they need to first upgrade the produced biogas to green gas before injecting it to the low pressure gas grid. Upgrading biogas to green gas is defined as the removal of CO_2, H_2S, H_2O, NH_3 from biogas [32]. As a result, the methane content of green gas is higher than 95%. The upgrading facility is shared by the community as it is easily seen that the costs change really fast with the scale [33].

Upgrading not only requires energy for the process itself, but also differences exist to what extent the process is able to separate the methane from other components (methane losses). The efficiency depends on the way of upgrading, from 75% to 91% [42].

2.2 Prosumers

The setup of one household is shown in Figure 2.2. As mentioned before, every prosumer is equipped with a μ-CHP device, fuelled on biogas [1]. The μ-CHP mainly consists of a **prime mover**, whose power and heat production are coupled, and an **auxiliary burner** which is capable only of heat production [7].
Every household is also equipped with gas and heat buffers. The first one is used to store the gas before using it and heat storage is used to fulfill the heat demand.

Parameter	Value	Unit
η_p, η_h	0.3, 0.7	-
P_{min},P_{max}	0, 3.0	kW
η_{aux}	1	-
H_{min},H_{max}	0, 20.0	kW

Table 2.1: Parameters of μ-CHP equipped with auxiliary burner according to [8]

Every household i has a local heat demand $H_{d,i}(t)$ and a local power demand $P_{d,i}(t)$ that can be measured at each time step t, where the heat demand is the aggregated space heating and domestic hot water needs. The main goal of the model consists of fulfilling these demands in the economically optimal way. There are two options in order to meet the demand of electric power: produce it with the prime mover, $P_{prod,i}(t)$, or buy it from the power grid at the price of the electricity market, $SP(t)$. On the other hand, to satisfy the heat demand, all the heat has to be produced by the μ-CHP (either in the prime mover, $H_{prod,i}(t)$, or in the auxiliary burner, $H_{aux,i}(t)$) and/or taken from the heat buffer. These energy productions are restricted by the physical parameters of

the μ-CHP (see Table 2.1).

Each μ-CHP has power, heat and auxiliary burner efficiencies, $\eta_{p,i}$, $\eta_{h,i}$ and $\eta_{aux,i}$ respectively, an associated operational cost $C_{CHP,i}(t)$ (mainly due to the prime mover) and a working range. The working range is defined by the production capacities of the prime mover and the auxiliary burner, being $P_{min,i}$ and $P_{max,i}$ the power production limits and $H_{min,i}$ and $H_{max,i}$ the auxiliary burner heat production limits. As stated before, the power production and the heat production of the prime mover are coupled, which makes the power production limitations also limitations in the heat production. Further information of this coupling is given in Chapter 3. Although these parameters may be different for each household installation, in this research it is assumed that all of them have the same values.

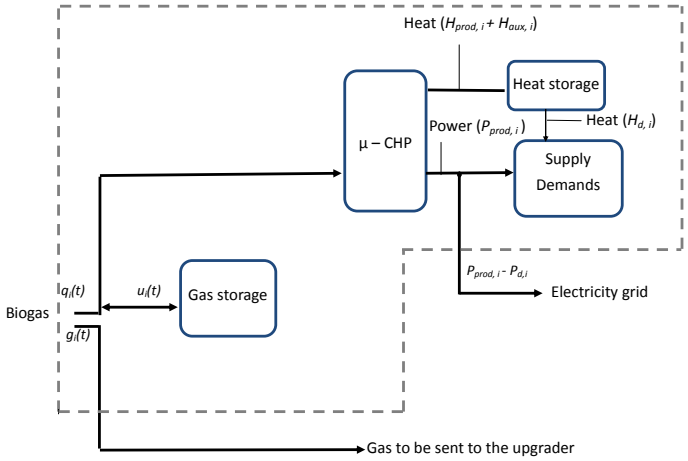

Figure 2.2: Scheme of a household equipped with μ-CHP and energy storage devices.

Once a prosumer receives the biogas from the digester, it has three options or a combination of them:

- store the biogas to its local gas storage device,
- send the biogas to the upgrader, in order to sell it immediately to the low pressure gas grid *or*
- turn the prime mover and/or auxiliary burner of μ-CHP on.

These choices will be made to optimize the estimated profit of each prosumer given the estimated selling price of electricity grid and the predicted selling price pof the

gas grid, while meeting its local heat and power demand. If the μ-CHP is turned on, a prosumer can decide at which level, inside the working range, should the μ-CHP work.

Furthermore, a prosumer can buy electricity to the power grid if the selling price in the power grid, $SP(t)$, is lower than the associated operational cost of the μ-CHP, $C_{CHP,i}(t)$. However, as mentioned before, its own heat demand ($H_{d,i}(t)$) has to be completely fulfilled. In order to achieve this, μ-CHP devices studied here have auxiliary burners that allow prosumers to produce extra-heat, $H_{aux,i}(t)$, not coupled with electricity production.

2.2.1 μ-CHP

The cogeneration is worldwide considered as the major option to achieve considerable energy saving with respect to traditional systems [43]. μ-CHP are the micro version of Combined Head and Power (CHP) devices. Such devices are considered *micro* when their electric power output is $\leq 15kW$, and, therefore, are applicable to small-scale users (residentials and light commercial application) [43].

μ-CHP can be relatively small and are expected to be of the same size as the current heating systems [7]. Compared to current heating systems, micro-CHP is a step forward in terms of energy efficiency [44]. By generating electricity locally and utilizing the coproduced heat, the efficiency of domestic energy use is substantially improved. In Figure 2.3, a comparison between a house with separate generation and a house with cogeneration (μ-CHP) is given, as well as the basic principle of the μ-CHP. Assuming that a household needs 20 units of electrical energy and 80 units of heat, and assuming a boiler efficiency of 100% and an efficiency of large power generation of 45%, a household consumes 124 units of primary energy in the case of separate heat and power generation. Alternatively, with the installation of a μ-CHP device of 20% electric and 80% thermal efficiency, 100 units of primary energy are required, leading to primary energy savings of around 20% [7].

In the recent years there has been significant progress toward developing kW-scale CHP applications. μ-CHP systems are on the verge of becoming mass marketed as a next generation domestic heating system [44] [45]. CHP generation system is considered nowadays as a major alternative to traditional energy systems in terms of lower CO 2 emissions as well as energy saving [47].

A simple layout of a μ-CHP installation is shown in Figure 2.4, using prime mover to satisfy the thermal and electrical needs of a residential building utilizing preinstalled conventional grid system. In the case where the production is higher than the demand, the excess energy can be sent to external electric network. Alternatively, if the demand is higher than the μ-CHP production, the external electric network can fulfill this energy shortage [46].

There are several types of prime mover technologies, which are under development, such as internal combustion engines (ICE), micro gas turbine (MGT), organic Rankine

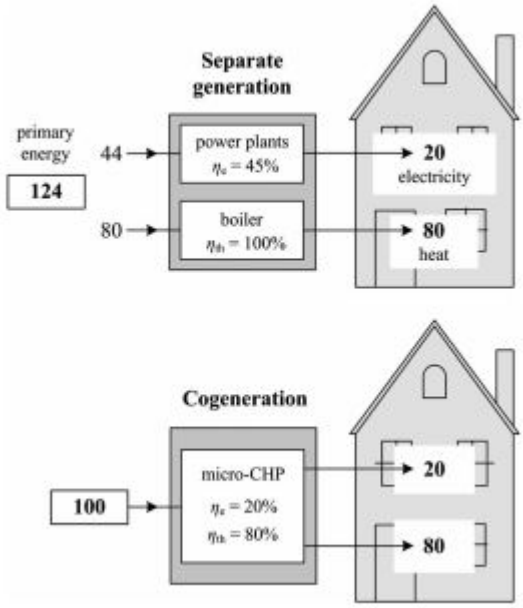

Figure 2.3: Comparison of efficiencies with and without a μ-CHP device [7]

cycle (ORC), thermophotovoltaic generators (TPVG), Stirling Engines (SE) and fuel cells [47] [48]. These technologies can work with different fuels giving out different amounts of electrical and thermal outputs.

The main difference between these technologies is the ratio of heat and electricity produced by the systems ranging from 5 (Stirling engine) to 0.8 (high temperature Fuel cell). Also different CHP systems determine the type of dwelling in which there are to be installed. Additionally, the efficiency of the CHP system is not only influenced by the type of fuel source being used but also by the type of prime mover technology. However, whichever technology is utilized, the efficiency of CHP system is always higher than the conventional or separated heat and power systems [47].

When comparing a conventional on-site coal-fired power plant along with gas boiler with an on-site CHP system, the second represents energy saving of up to 30%. Energy efficiency of 100% can be obtained with micro-cogeneration. Furthermore, distributed CHP system reduces the primary energy consumption and increase the site energy consumption. It is reported in the literature that all the available CHP technologies give CHP efficiency not less than 75%, increasing energy reliability for the user. Besides this, CHP technologies are well known due to their efficient CO_2 saving as compared to conventional grid electrical network. Different CHP prime mover technologies offer

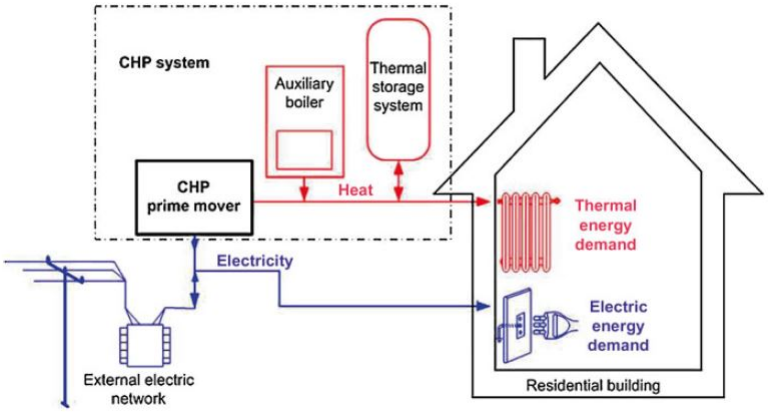

Figure 2.4: Simple layout of a μ-CHP device [46]

different range of CO_2 saving capabilities ranges from 0.50 to 0.85 tons per annum (t/a) [46].

Type of CHP system	Capacity kW	Electrical output (kW_e)	Thermal output (kW_t)	Electrical efficiency (%)	Thermal efficiency (%)	CO_2 saving (ratio)
ICE	1–100	1–13	3–29	20–26	60–70	0.8
MGT	30–250	30	–	33	60	0.5
ORC	100–200	1–10	8–44	6–20	70–80	0.5
TPVG	–	1.5	12.2	<15	75	0.7
SE	50–250	1–9	5–25	13–28	60–80	0.65
FC	5–200	1–4.6	0.521–2	52	30–40	0.85

Table 2.2: Main characteristics of prime mover technologies [46]

In Table 2.2, the list of characteristics of each technology is given. In this work it is chosen that all devices will be Proton Exchange Membrane Fuel Cell (PEMFC) because of the high electricity efficiency of this technology. However, this is not the only advantage of this technology: as stated in [46], this technology produces lower level of emissions, lower level of noise and is easier to use compared to other CHP systems.

2.2.2 Gas storage

According to [31], there are two main reasons for gas storage, namely short-term fluctuations in demand and different needs in each season. This is to say that, since the production of an anaerobic digester is a more or less constant process, it is necessary to have a small storage device to meet the demand for every time step t. The other reason for gas storage is long-term storage of gas due to annual cycle in gas use, i.e. in winter,

the use of gas is 6-10 times higher than in summer.

The least expensive and easiest to use storage systems for on-farm applications are low-pressure systems; these systems are commonly used for on-site, intermediate storage of biogas. The energy, safety, and scrubbing requirements of medium and high pressure storage systems make them costly and high maintenance options for an on-farm use. Table 2.3 briefly shows the different options for biogas storage [32].

Purpose of Storage	Pressure (psi)	Storage Device	Material	Size (ft^3)
Short and intermediate storage for on-farm use (currently used on farms for biogas storage)	< 0.1	Floating Cover	Reinforced and non-reinforced plastics, rubbers	Variable volume usually less than one day's production
	<2	Gas bag	Reinforced and non-reinforced plastics, rubbers	150 – 11,000
	2 – 6	Water sealed gas holder	Steel	3,500
		Weighted gas bag	Reinforced and non-reinforced plastics, rubbers	880 – 28,000
		Floating roof	Plastic, reinforced plastic	Variable volume, usually less than one day's production
Possible means of storage for later on- or off-farm use (could be used for biomethane)	10 – 2,900	Propane or butane tanks	Steel	2,000
	>2,900	Commercial gas cylinders	Alloy steel	350

Table 2.3: Different options for biogas storage in the households [32].

2.2.3 Heat storage

As explained before, local heat demand has to be completely fulfilled by each prosumer. This makes necessary to have the capacity to store heat to meet the mismatch between demand and production at any time. Among all the commercially available storage systems, cylindrical hot water tanks are the most extended solution and have been widely considered as a way of boosting the profitability of μ-CHP systems [22]. The energy losses can be neglected [34] and are expected not to influence the results of the analysis presented [7]. The working range for the storage is given by

$$\begin{aligned} h_{min,i} &= m_i \cdot c_p \cdot \Delta T_{min,i}, \\ h_{max,i} &= m_i \cdot c_p \cdot \Delta T_{max,i}. \end{aligned} \tag{2.1}$$

where m is the mass of the water and c_p is the specific heat constant. ΔT is the difference between the room temperature and T_{max} or T_{min}. T_{max} is assumed to be $80^{\circ}C$ and T_{min} is assumed $55^{\circ}C$ for all the prosumers. It is also assumed that all prosumers use the same type of heat storage with a mass of water from $100l$ to $200l$ [7]. Some simulations will be run to see how the size affects the performance.

2.3 External energy grids

As explained before, each household is connected to the same low pressure gas grid and the same power grid. This section explains what is their function in the studied systems and the main characteristics of both grids in the Netherlands.

The low pressure gas grid has one function when interacting with the system, i.e. it is used to sell the biogas that is not going to be used nor stored, adn therefore, to create revenue from excess biogas. The power grid has two functions in this work, which are: 1) fulfill the power demand when the production is not enough (or when the grid price is lower than the production price), and 2) sell the excess electricity to get some revenue.

2.3.1 Low pressure gas grid

Gasunie provides the transport of natural gas and green gas in the Netherlands and the Northern part of Germany. Gas is an important source of energy in northwest Europe. To get the gas to the end-user safely and reliably, Gasunie has a high-grade gas transmission grid. Their customers use this grid to transport gas on to end-users and some end-users are directly connected to the grid. The subsidiary that manages the Dutch gas transmission grid is Gasunie Transport Services (GTS).

2.3.2 Electricity grid

In the Dutch liberalized electricity market, balancing is the responsibility of the so-called Programme Responsible Parties (PRPs). Every generator and load in the Netherlands is assigned to a PRP who are responsible towards the Transmission System Operator, TenneT, to maintain the scheduled quarter-hourly energy exchange with the Dutch system of all generators and load in their portfolio. Deviations from the schedule are penalized by the TSO (imbalance-pricing) [21].

2.4 System boundaries

The system described above is studied within some boundaries. These boundaries and their consequences are briefly explained in this subsection.

The management of agricultural wastes is not studied in detail. The biogas from agricultural wastes is taken directly from the digester. We develop the math model of electricity grid and the low pressure gas grid mainly based on the dynamics of the capacity levels and the selling price at every time instant t. Moreover, we assume that every prosumer has exact prediction of its local heat and power demand, and every operator and/or central controller has exact prediction of biogas availability and price and capacity of the electricity and gas grids in a given prediction horizon.

At last, the prime mover has a relatively long start-up time when it has been shut down. During this period an amount of gas is consumed, but no electricity and a neglectable amount of heat are produced. If the prime mover is frequently shut down, this could limit the opportunity to control the power output. A choice can therefore be to keep the prime mover at an idle on-state, in which state the prime mover can resume production at any time. Nevertheless, in an idle on-state, the prime mover consumes the minimum gas amount g_i, r, required to keep the reforming unit at the operating temperature, even if no power and heat are produced. This minimum gas amount used is not used in the model since it is constant and, therefore, does not affect the results.

2.5 Control objective

In this section, the literature research has its goal in finding a suitable control algorithm for the previously presented system.

The desired control is meant to be a real-time process, able to take predictions into account as well as the constraints and the dynamics of the system. The controller must optimize over a prediction horizon, while complying all the technical and dynamic constraints. Multiple control systems that are suitable for such a smart grid are proposed in [23]. The research on production and demand control mainly consists of (a combination of) optimization methods, game theory, machine learning and auction methods [54]. In this subsection, we introduce the concept of these methods and some examples of each are given.

Optimization methods calculate the optimal decisions regarding energy usage based on given inputs and disturbances and satisfying particular constraints. The optimal decisions are based on a pre-defined objective, like minimizing costs or maximizing profit. Different optimizations can in [35] for convex programming, in [36] for dynamic programming, in [37] for stochastic programming, in [38] for robust programming and in [39] for particle swam optimization.

Game theory studies decision making of individuals and groups, based on mathematical models. One of the areas of game theory is non-cooperative games, in which the users only focus on achieving their own goals, instead of cooperating to a common goal. A special solution concept in non-cooperative game is the **Nash equilibrium**, in which all players achieve an optimal solution, taking into account the solution of others. Our system could be seen as a non-cooperative game and, with the help of game theory, the model can be designed such that the set of optimal solutions of each household lead to an optimal solution for the system as a whole [25].

Machine learning is a field of study in Artificial Intelligence that focuses on the learning of computers based on empirical data. The computer is encouraged to be programmed in such a way that, based on previous experiences, it acts accurately in a new situation. To do so, the algorithm behind it needs to identify complex links that underlay the empirical data, to predict the behaviour when parameters change. In application

to our system, machine learning could, for example, be used to estimate the effect of some decisions of households about their device use [26].

Auction is the process of buying and selling with help of price bids; different users make bids on products/services and the auctioneer decides which items are sold to which bidders. This market mechanism is used in our case to make supply and consumption bids to the operators of the power grid, the gas grid and biogas producer [24].

In this research, a combination of optimization, game theory and auction is implemented in order to try to achieve the Nash equilibrium.

Requirements of the control system

The control system requires some requisits, i.e.

- It must maximize the estimated profit of prosumers
- It must comply all the constraints and take predictions into account.
- It must have low computational load.
- There has to be the possibility of distributed control due to the fact that we want prosumers to be as independent as possible when making the decisions.

The most suitable method that meets all these requirements is **MPC** [27].

2.5.1 MPC

Model Predictive Control (MPC) is an advanced type of process control. It can control a dynamical system by minimizing or maximizing its objective while meeting the model's constraints. MPC uses the current variables of the system and a prediction of the future to calculate next time steps. Only the first calculated time-step will be implemented in the system, and then the optimization process will start again from the following time-step (see Receding Horizon Principle, in section 3.2.6). Significant progress has been made in understanding the behaviour of MPC systems, and a lot of results have been obtained on stability, robustness and performance of MPC. [41]

The main conveniences of MPC are that it can be used to handle multivariable control programs, operates in real time, optimizes over a prediction horizon, is able to include constraints and to offer distributed control [27].

In this work, MPC is used to control the grid of prosumers and its relation with the operators of the gas grid, the electricity grid and the biogas producer. The goal is the maximization of the estimated profit for every prosumer while respecting all the technical constraints. Predictions are used for heat and power demands and for the available amount of biogas, as well as for the information on the gas and power grid about capacity and price.

Distributed MPC (DMPC)

The centralized setup has some advantages, but also some drawbacks, like high computational load when the number of prosumers is high, and the certainty that if there is a failure, all system will be down, as examples. That is why, in most cases, it is recommended to use a distributed controller, which gives the possibility to every prosumer to optimize its own problem. It also reduces the computational load of the model and solve some issues on reliability, as well as decentralized the problems in case of failure. Dual decomposition combined with the subgradient method is used in order to obtain the DMPC from the (centralized) MPC [19]. In [17] and in [18], examples for distributed model predictive for multiple systems are given as well as stopping criteria that ensure closed loop iterations.

Chapter 3

Controller Design

In this chapter the controller is designed. Firstly, an overview of the design procedure is presented. Next, the model itself is presented in the centralized and distributed manners. Thirdly, the convergence of the model is studied and, at the end of the chapter, an explanation on how the optimization will be performed is given.

3.1 Design Procedure

For every MPC controller design there are several ingredients that form the basis of the MPC design procedure [54]. These ingredients are briefly described in this section.

1. **Disturbance and process model**: A disturbance model describes how the output of the model behaves as a result of input and disturbance to the model [54]. A process model describes how the process variables for the given horizon can be predicted.

2. **Performance index**: The main performance index, also called objective function, is the total estimated profit for the prosumers. The purpose of the control mechanism is to maximize it.

3. **Constraints**: They include all the physical limitations and characteristics of the model that restrict the objective function. In our case, this is to say that it includes the technical constraints on prosumers' devices, on the capacities of gas and power grids and on the biogas availability of the biogas producer.

4. **Optimization**: A technique to find the best control sequence that maximizes the estimated profit.

5. **Receding horizon principle**: It is a method used so the model can adapt to all the unexpected future events.

All these steps will be explained further in the following sections.

3.2 Model

In this section the problem is modeled. First, the controllable variables will be exposed. Secondly, the centralized approach will be presented and, finally, the distributed approach will be explained. In both cases, the chosen approach is the heat demand driven model. This is to say that the heat demand always needs to be fulfilled at any time, by maintaining the storage level inside a determined range [8].

3.2.1 Controllable variables

The controllable variables, or controllable inputs are those that can be modified or chosen by the controller. In this system there are four controllable inputs:

- $H_{prod,i}(t)$: The heat production by the prime mover. It can be adjusted within the working range of the μ-CHP which, as explained before, is related to the power production $P_{min,i}$ and $P_{max,i}$, and which is coupled to the heat production. This coupling is further explained in next subsection. $H_{prod,i}(t) \geq 0$.
- $H_{aux,i}(t)$: The heat production by the auxiliary burner. It can be adjusted within the working range of the μ-CHP, $0 \leq H_{aux,min,i}$ and $H_{aux,max,i}$.
- $g_i(t)$: The biogas to be sent to the upgrader before selling it to the low pressure gas grid. $g_i(t) \geq 0$.
- $u_i(t)$: The interaction with the gas storage, either adding gas, $u_i(t) \in R_+$, or taking it out, $u_i(t) \in R_-$.

3.2.2 Centralized problem

In this section, the centralized approach is presented. This perspective assumes that there is a central controller, with all the information of the system, that decides the best production plan for every prosumer i.

Constraints

μ-CHP technical constraints As mentioned before, heat and power production of the prime mover of the μ-CHP are coupled. This coupling is given by

$$H_{prod,i}(t) = \frac{\eta_{h,i}}{\eta_{p,i}} \cdot P_{prod,i}(t) \tag{3.1}$$

This levels of production are limited to a working range according to

$$P_{prod,i}(t) \in [P_{min,i}, P_{max,i}]. \tag{3.2}$$

The auxiliary burner can be turned on to provide heat $H_{aux,i}(t)$ when there is a high heat demand or when it is more profitable to not produce the electricity (because the operational cost of the μ-CHP, $C_{CHP,i}(t)$ is higher than the price of electricity in the spot market, $SP(t)$). Its working range is given by

$$H_{aux,i}(t) \in [H_{min,aux,i}, H_{max,aux,i}]. \tag{3.3}$$

Heat storage constraints It is assumed that there are no thermal losses in the conversion and storage system. Thus, the dynamics of the heat storage level $z_{h,i}(t)$ are defined by

$$z_{h,i}(t+1) = z_{h,i}(t) + H_{prod,i}(t) + H_{aux,i}(t) - H_{d,i}(t). \tag{3.4}$$

In order to completely fulfil the heat demand, the following constraint must be met in every time step.

$$h_{min,i} \leqslant z_{h,i}(t) \leqslant h_{max,i} \tag{3.5}$$

meaning that the level of heat storage has to be always inside the range. $h_{min,i}$ and $h_{max,i}$ are given by

$$\begin{aligned} h_{min,i} &= m_i \cdot c_p \cdot \Delta T_{min,i}, \\ h_{max,i} &= m_i \cdot c_p \cdot \Delta T_{max,i}. \end{aligned} \tag{3.6}$$

where m is the mass of the water and c_p is the specific heat constant. ΔT is the difference between the room temperature and T_{max} or T_{min}.

Gas storage Assuming that there are no leaks in the gas storage, its dynamics are modelled as

$$z_{g,i}(t+1) = z_{g,i}(t) + u_i(t) \tag{3.7}$$

where $z_{g,i}(t)$ denotes the level of storage and $u_i(t)$ denotes the gas that is added to the storage ($u_i(t) > 0$) or taken from the storage ($u_i(t) < 0$). There is a maximum capacity, $G_{cap,i}$, and the constraint is defined as

$$0 \leq z_{g,i}(t) \leq G_{cap,i} \tag{3.8}$$

Therefore, the range of u, the variable associated at the interaction with the biogas storage, is defined by:

$$-z_{g,i}(t) \leq u_i(t) \leq G_{cap,i} - z_{g,i}(t) \tag{3.9}$$

Biogas consumption Assuming that the losses of the μ-CHP are negligible, the biogas used by every prosumer i, $q_i(t)$, is defined by

$$q_i(t) = \frac{H_{prod,i}(t)}{\eta_{h,i}} + \frac{H_{aux,i}(t)}{\eta_{aux,i}} + u_i(t). \tag{3.10}$$

Coupling constraints

So far, the constraints from 3.1 to 3.10 are applied to each prosumer separately. In fact, there are three constraints that are applied to all of them as a set. These are the coupling constraints.

First, there is a limited amount of biogas available, $B(t)$, for all prosumers. Each prosumer can sell the biogas ($g_i(t)$) or use it ($q_i(t)$).

$$\sum_{i=1}^{n} q_i(t) + g_i(t) \leq B(t), \tag{3.11}$$

where $g_i(t)$ denotes the amount of biogas that is upgraded before selling it to the low pressure gas grid.

Secondly, the capacities of the gas and electric grids cannot be exceeded by the amount of biogas and electricity sold by the prosumers. This translates into the following constraints

$$\sum_{i=1}^{n} P_{prod,i}(t) - P_{d,i}(t) \leq EG_{cap}(t). \tag{3.12}$$

$$\sum_{i=1}^{n} g_i(t) \leq GG_{cap}(t). \tag{3.13}$$

where $EG_{cap}(t)$ stands for the amount of electricity that the power grid can absorb and $GG_{cap}(t)$ stands for the amount of biogas that the gas grid can absorb.

Objective Function

The objective is to maximize the total estimated profit for n prosumers at a given time horizon T. The maximization is done over the set of controllable variables $\nu = \{H_{prod,i}(t), H_{aux,i}(t), g_i(t), u_i(t)\}$.

$$\begin{aligned} \max_{\nu} \sum_{i=1}^{n} \sum_{t}^{T} H(\nu) &= \max_{\nu} \sum_{i=1}^{n} \sum_{t}^{T} (SP(t) - C_{CHP,i}) \cdot (P_{prod}(i,t) - P_d(i,t)) \\ &- c_{tp,i}(t) \cdot (P_{prod}(i,t) - P_d(i,t))^2 + (GP(t) - c_{g,i}(t)) \cdot \eta_{upgr} \cdot g_i(t) \\ &- c_{tg,i}(t) \cdot \eta_{upgr} \cdot g_i(t)^2 - w \cdot u_i(t)^2 - y \cdot H_{aux,i}(t)^2 \end{aligned} \tag{3.14}$$

where $c_{tp,i}(t)$ is the cost associated with transmission losses when interacting with the power grid, $c_{g,i}(t)$ is the cost of producing and selling green gas to the low pressure gas grid, η_{upgr} is the efficiency of the process of upgrading the biogas to green gas, $c_{tg,i}(t)$ is the cost associated with transmission losses of $g_i(t)$, and w and y are weighting factors of the effort in storing and using biogas from the storage and the importance of the heat produced in the auxiliary burner, respectively. The transmission losses are formulated with quadratic function as in [49].

3.2.3 MPC framework

The optimization problem presented in 3.14 is solved in MPC framework. With this framework, the profit is maximized over a time horizon K given the estimations of future conditions in the power grid, the low pressure gas grid, the biogas production level, and the local heat and power demands. From the sequence of optimal solutions that covers the time horizon K, only the calculated solution of the first step is applied. At the next time step, the optimization problem is re-solved, but again, only the first step is applied.

This helps prosumers to have a better management on their supply and consumption levels. It also helps the operators of the grids and the biogas producer to avoid overloading the grids or biogas shortage, respectively.

Therefore, the centralized problem is stated as follows.

$$\max_{v} \sum_{i=1}^{n} \sum_{\tau=1}^{K} \hat{H}(v(\tau)) \tag{3.15}$$

subject to the prediction model of the constraints explained before.The hat notations are the prediction variables.

3.2.4 Distributed MPC

The drawback of the presented centralized model is that there is the need for a central operator to control the interactions with the external part of the system, i.e the gas and power grids and the biogas producer, and this decreases the capacity of decision of every prosumer i. In addition, it is easy to see that the number of variables to be calculated grows fast as the size of the grid increases. Therefore, the computational load for solving the model also gets larger.

This section approaches the problem from a distributed point of view, meaning that every prosumer i solves his own optimization problem. This way, the problem will be solved using updates of the Lagrange multipliers of the dual problem and a stopping criterion, based on [17]. In this case, however, it is not possible to get a fully distributed model, because there is the need of a central grid operator to avoid overloading grids.

Dual problem

The centralized model presented previously will be, then, converted into a distributed one on the basis of a dual decomposition. In the dual optimization problem, the coupling constraints are added to the objective function with a specific weight. These weights are known as Lagrange multipliers, see [19].

In order to get the distributed model, the problem will be formulated for each prosumer i. As explained in the centralized model, there are several constraints that apply to all the prosumers as a set, i.e. the coupling constraints. These constraints are:

$$\sum_{i=1}^{n} q_i(t) + g_i(t) \leq B(t), \tag{3.16}$$

$$\sum_{i=1}^{n} P_{prod,i}(t) - P_{d,i}(t) \leq EG_{cap}(t). \tag{3.17}$$

$$\sum_{i=1}^{n} g_i(t) \leq GG_{cap}(t). \tag{3.18}$$

Since there are three coupling constraints, three Lagrange multipliers will be used respectively: λ, μ and α, which are all nonegative values. The dual decomposition is used to formulate the Lagrange dual function L. The Lagrange function is based on the centralized objective function, but it also includes the coupling constraints weighted by the Lagrange multipliers.

$$
\begin{aligned}
L &= \sum_{i=1}^{n}\sum_{\tau=1}^{K}(\hat{SP}(\tau)-C_{CHP,i})\cdot(\hat{P_{prod,i}}(\tau)-\hat{P_{d,i}}(\tau))-\hat{c_{tp,i}}(\tau)\cdot(\hat{P_{prod,i}}(\tau)-\hat{P_{d,i}}(\tau))^2 \\
&+ (\hat{GP}(\tau)-\hat{c_{g,i}}(\tau))\cdot\hat{g}_i(\tau)-\hat{c_{tg,i}}(\tau)\cdot\hat{g}_i(\tau)^2-w_i\cdot\hat{u}_i(\tau)^2-v_i(\tau)\cdot\hat{H_{aux,i}}(\tau)^2 \\
&- \hat{\lambda}_i(\tau)\cdot(\sum_{i=1}^{n}(\hat{q}_i(\tau)+\hat{g}_i(\tau)-\hat{B}(\tau))-\hat{\mu}_i(\tau)\cdot(\sum_{i=1}^{n}\hat{P}_{prod,i}(\tau)-\hat{P}_{d,i}(\tau)-\hat{EG}_{cap}(\tau)) \\
&- \hat{\alpha}_i(\tau)\cdot(\sum_{i=1}^{n}\hat{g}_i(\tau)-\hat{GG}_{cap}(\tau)) \qquad (3.19)
\end{aligned}
$$

The maximization of L becomes the function $F(\hat{\lambda},\hat{\mu},\hat{\alpha})$, which gives lower bounds on the optimal value of the original optimization problem. The original problem, the centralized, will be called from now on *primal problem*. The objective function of the dual problem, then, is

$$F(\hat{\lambda},\hat{\mu},\hat{\alpha})=\max_{\hat{v}}L(\hat{v},\hat{\lambda},\hat{\mu},\hat{\alpha}). \qquad (3.20)$$

where $\hat{v}$ is the subset of controllable inputs of the system, namely $\hat{H}_{prod,i}(\tau)$, $\hat{H}_{aux,i}(\tau)$, $\hat{u}_i(\tau)$ and $\hat{g}_i(\tau)$.

So far, the primal problem with coupled constraints has been converted to a dual problem with a coupled objective function, but with non-coupled constraints. This problem can still only be solved in a centralized setting. In [17] it is proven that this coupled objective function is equivalent to:

$$\min_{\hat{\lambda},\hat{\mu},\hat{\alpha}}F(\hat{\lambda},\hat{\mu},\hat{\alpha})=\min_{\hat{\lambda},\hat{\mu},\hat{\alpha}}\sum_{i=1}^{n}\max_{\hat{v}_i}L(\hat{v},\hat{\lambda},\hat{\mu},\hat{\alpha}) \qquad (3.21)$$

This new objective function has an inner maximization problem (F) that is fully decoupled of the grids and the biogas producer, which can be solved by MPC, with given values of $\hat{\lambda}$, $\hat{\mu}$ and $\hat{\alpha}$. Optimization can be performed, therefore, by each node separately.

For given values of the Lagrange multipliers, the output of the optimization gives the lower bound on the optimal value of the primal problem. To find the best set of lower bounds, the dual function is maximized over the Lagrange multipliers, which has to be done in a centralized manner. The Lagrange multipliers can be optimized easily using iterative processes. The authors in [17] propose to coordinate this optimization by finding the optimal values as limits of a gradient iteration. Based on their proposal, the distributed optimization start with some initial values for the Lagrange multipliers and they update the multipliers using gradient steps given by

$$\hat{\lambda}^{r+1}(\tau) = \hat{\lambda}^{r}(\tau) + \hat{\gamma}_i^r(\tau)\left(\sum_{i=1}^{n}(\hat{q}_i^r(\tau) + \hat{g}_i^r(\tau)) - \hat{B}(\tau)\right) \tag{3.22}$$

$$\hat{\mu}^{r+1}(\tau) = \hat{\mu}^{r}(\tau) + \hat{\varepsilon}_i^r(\tau)\left(\sum_{i=1}^{n}(P_{prod,i}^r(t) - P_{d,i}(t)) - EG_{cap}(t)\right) \tag{3.23}$$

$$\hat{\alpha}^{r+1}(\tau) = \hat{\alpha}^{r}(\tau) + \hat{\beta}_i^r(\tau)\left(\sum_{i=1}^{n}\hat{g}_i^r(\tau) - \hat{GG}_{cap}(\tau)\right) \tag{3.24}$$

where $\hat{\gamma}_i^r(\tau)$, $\hat{\varepsilon}_i^r(\tau)$ and $\hat{\beta}_i^r(\tau)$ are sufficiently small step sizes. The variable r represents the number of the gradient iteration. Convergence of such gradient algorithms has been proved under different types of assumptions on the step size sequence $\hat{\gamma}_i^r$, $\hat{\varepsilon}_i^r$ and $\hat{\beta}_i^r$ [17]. In particular the following non-summable diminishing step size is chosen [20]:

$$\hat{\gamma}_i^r(\tau) = \frac{\delta \cdot \hat{a}(\tau)}{\sqrt{r}} \tag{3.25}$$

$$\hat{\varepsilon}_i^r(\tau) = \frac{\delta \cdot \hat{SP}(\tau)}{\sqrt{r}} \tag{3.26}$$

$$\hat{\beta}_i^r(t) = \frac{\delta \cdot \hat{GP}(\tau)}{\sqrt{r}} \tag{3.27}$$

where $\delta = 0,00055$ for which convergence is proven by any $a(t), SP(t), GP(t) > 0$ given that the optimization problem is convex. Since the model is convex, strong duality is assured by the KKT conditions.

The updates of the Lagrangian multipliers are done by every operator (i.e. biogas producer, electric grid operator, and gas grid operator) with all the information and bids from the prosumers. Once the multipliers are updated, the new values can be used as input for the distributed optimization problem.

The Lagrangian multipliers in the dual problem are often interpreted as prices or shadow prices. This interpretation comes from economics and game theory literature [19].

3.2.5 Synchronous and Asynchronous approaches

As explained in the previous sections, the problem is solved in a distributed manner, where each prosumer can make a decision on their own supply and consumption levels, based on their local information and some coordination with the operators. Practically, the agents and operators may not have a common clock to synchronize their updates. Therefore, we will simulate both scenarios: the *synchronous*, where they both have the same clock to update their information exchange and an *asynchronous* model, where they cannot have an access to a common clock.

In the asynchronous model, both the prosumers and operators will adjust their decision variables according to their current knowledge of others information. On the one hand, the operator will adjust its Lagrangian multiplier $\lambda^r(t)$ based on its current knowledge of the aggregated supply levels from all prosumers $i \in I$ where $I = 1, ..., n$. On the other hand, the prosumer will estimate a Lagrangian multiplier for every time step where they do not have information from the operators.

3.2.6 Interpretation of the distributed model: Interaction between operators of the grids and prosumers

The interacting agents participating are the prosumers, who utilize the gas and electricity distribution grids and the biogas generator, and the operators of each of these, who are responsible for meeting the grid capacity constraints. From now on, the operators of both grids (electricity and gas) and the operator of the biogas generator will be called *Operators of the System* (OS).

Based on these shadow prices and based on information regarding storage level, production level, demands, selling prices and the prediction of each of these, each prosumer locally optimizes their supply and consumption levels. The prosumers then inform the OSs of their bids on production and consumption levels, under the initial shadow prices. By summing all the bids, each OS determines if the grid is overloaded or underloaded; or, in the case of the biogas producer, the capacity is exceeded or not, which behaves as an overloaded/underloaded grid. When a grid is overloaded, the shadow price is increased, and when a grid is underloaded the price is decreased, according to the presented algorithm. Nonetheless, the shadow prices have to be non-negative and are identical for all prosumers on the grid. Since the shadow prices are initiated at zero the OSs will increase the shadow prices if necessary to prevent overloading the grids. This is done until the increase in shadow price is smaller than a predefined threshold value which indicates that the optimum is approached.

The shadow price can be seen as a virtual price that the prosumers have to pay to the operators for their bids: a shadow price of 0 indicates that bids are not reaching the maximum capacity of the grids, so it is still cheap to bid some more. A larger shadow price is the consequence of desired bids exceeding available capacity, so it is more virtually expensive for the prosumers to bid, and they will reduce the bids. As a result, the prosumers will reach the global optimum (within the horizon). When the increase/decrease of the shadow price is sufficiently small the OS terminate the iterations.

Receding Horizon Principle

MPC makes use of the receding horizon principle. This is to say that, after optimizing over the given horizon, only the first control input of the computed sequence will be implemented. After this implementation, at the next time step, a new optimization over the given horizon will be made and, once again, only the first control input will be implemented. The prediction horizon of the new optimization problem is shifted one

time step and new predictions are implemented.

The basis of receding horizon principle is shown in figure 3.1. The upper image of this figure shows the first optimization process, which is done over the horizon period $t + t_r$. Once the optimization is done, only the first result is implemented in reality (red zone). In the following time step $t + 1$, optimization will be done again over a prediction horizon of the same length, moved one time step forward.

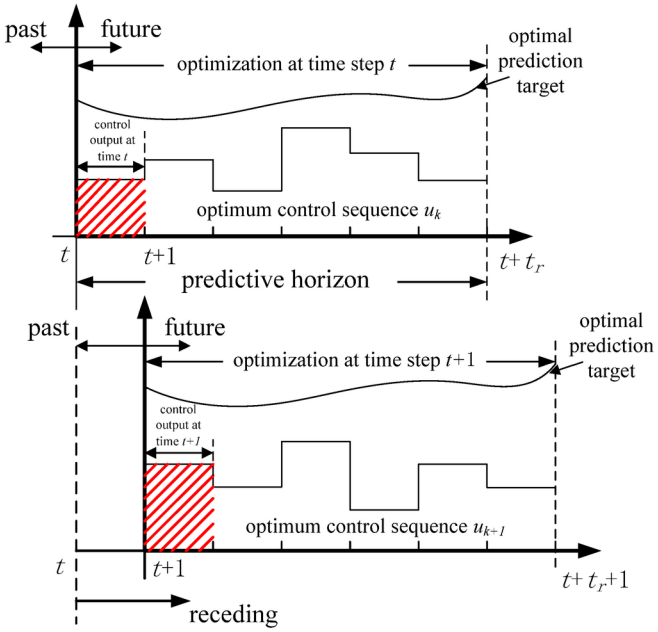

Figure 3.1: Basis of the Receding Horizon Principle [52]

3.3 Optimization

The performance index of this optimization problem is chosen to be quadratic and all constraints have been formulated as linear expressions. Therefore, the optimization is called linear *quadratic program*. The choice of method to solve a quadratic program depends on the type of constraints the model is subjected to. In this case, we have defined both equality and inequality constraints so the program is classified as *inequality constrained maximization problem*. By changing the sign of the objective function, we can get a minimization problem, and then we have an inequality constrained *minimization* problem. In [19], different methods to solve this category of programs are discussed.

3.4 Algorithm

In the previous chapter, two different controllers have been designed: centralized MPC and distributed MPC. We formulate the associated algorithms in the following subsections. The hats stand for the results of the optimization algorithm applied to a certain prediction horizon.

3.4.1 Centralized MPC

1. **Update** the predictions of the heat and power demands ($H_{d,i}(t)$ and $P_{d,i}(t)$), the available biogas ($B(t)$) and the capacities and prices of electricity and gas grids, i.e. $EG_{cap}(t)$, $GG_{cap}(t)$, $SP(t)$ and $GP(t)$.

2. **Optimization** of the problem presented in section 3.2.2 subject to all the constraints exposed in section 3.2.2.
   Initial conditions
   $\hat{z}_{h,i}(1) = z_{h,i}(t)$
   $\hat{z}_{g,i}(1) = z_{g,i}(t)$

3. **Implement** the first of the computed sequence of control actions (thus applying receding horizon principle).
   $H_{prod,i}(t+1) = \hat{H}_{prod,i}(1)$
   $H_{aux,i}(t+1) = \hat{H}_{aux,i}(1)$
   $u_i(t+1) = \hat{u}_i(1)$
   $g_i(t+1) = \hat{g}_i(1)$

4. **Calculate** the state variables at the time step $t = 1$ and $P_{prod,i}(t)$.
   $P_{prod,i}(1) = \frac{\eta_{p,i}}{\eta_{h,i}} \cdot \hat{H}_{prod,i}(1)$
   $z_{h,i}(2) = z_{h,i}(1) + \hat{H}_{prod,i}(1) + \hat{H}_{aux,i}(1) - H_{d,i}(1)$
   $z_{g,i}(2) = z_{g,i}(1) + \hat{u}_i(1)$
   $q_i(1) = \frac{\hat{H}_{prod,i}(1)}{\eta_h} + \frac{\hat{H}_{aux,i}(1)}{\eta_h} + \hat{u}_i(1)$

5. **Restart** from step 1 with the next time-step.

3.4.2 Distributed MPC

1. **The operators update** the predictions of the heat and power demands ($H_{d,i}(t)$ and $P_{d,i}(t)$), the available biogas ($B(t)$) and the capacities and prices of electricity and gas grids ($EG_{cap}(t)$, $GG_{cap}(t)$, $SP(t)$ and $GP(t)$).

2. Set initial Lagrangian multipliers $\lambda^{r=0}(t)$, $\mu^{r=0}(t)$ and $\alpha^{r=0}(t)$.

3. **Optimization.** Given $\lambda^r(t)$, $\mu^r(t)$ and $\alpha^r(t)$, each prosumer solves the optimization problem presented in section 3.2.4 subject to the prediction models of the constraints in section 3.2.2.

Initial conditions
$\hat{z}_{h,i}(1) = z_{h,i}(t)$
$\hat{z}_{g,i}(1) = z_{g,i}(t)$

4. **The operators update** Lagrangian multipliers with the step size defined in section 3.2.4.

$$\begin{aligned}
\lambda^{r+1}(t) &= \lambda^r(t) + \gamma_i^r(t)\left(\sum_{i=1}^{n}(q_i^r(t) + g_i^r(t)) - B(t)\right) \\
\mu^{r+1}(t) &= \mu^r(t) + \varepsilon_i^r(t)\left(\sum_{i=1}^{n}(P_{prod,i}^r(t) - P_{d,i}(t)) - EG_{cap}(t)\right) \\
\alpha^{r+1}(t) &= \alpha^r(t) + \beta_i^r(t)\left(\sum_{i=1}^{n} g_i^r(t) - GG_{cap}(t)\right)
\end{aligned}$$

5. **If** $\lambda_i^{r+1} - \lambda_i^r <= \delta$ and $\mu_i^{r+1} - \mu_i^r <= \delta$ and $\alpha_i^{r+1} - \alpha_i^r <= \delta$, and all the coupling constraints are met, go to next step. Else, go to step 3.

6. **Implementation** by the prosumers of the first of the computed sequence of control actions (thus applying receding horizon principle).
$H_{prod,i}(t+1) = \hat{H}_{prod,i}(1)$
$H_{aux,i}(t+1) = \hat{H}_{aux,i}(1)$
$u_i(t+1) = \hat{u}_i(1)$
$g_i(t+1) = \hat{g}_i(1)$

7. **Calculation** by the prosumer of the state variables at the time step $t = 1$ and $P_{prod,i}(t)$.
$P_{prod,i}(1) = \frac{\eta_{p,i}}{\eta_{h,i}} \cdot \hat{H}_{prod,i}(1)$
$z_{h,i}(2) = z_{h,i}(1) + \hat{H}_{prod,i}(1) + \hat{H}_{aux,i}(1) - H_{d,i}(1)$
$z_{g,i}(2) = z_{g,i}(1) + \hat{u}_i(1)\ q_i(1) = \frac{\hat{H}_{prod,i}(1)}{\eta_h} + \frac{\hat{H}_{aux,i}(1)}{\eta_h} + \hat{u}_i(1)$

8. **Restart** from step 1 with the next time-step.

3.4.3 Distributed MPC with asynchronous implementation

As explained before, asynchronous implies that not all the agents have access to the same clock. In this work, it is decided to study the case only for one operator using a different clock, which is the biogas producer. For implementing the asynchronous algorithm it is assumed that the prosumers send their bids to the operator of the biogas every iteration whose number is even. And the operator of the biogas producer sends the updated value of λ at every iteration whose number is odd.

Therefore, both prosumers and operators will have to estimate some values. The algorithm is implemented as follows.

1. **The operators update** the predictions of the heat and power demands ($H_{d,i}(t)$ and $P_{d,i}(t)$), the available biogas ($B(t)$) and the capacities and prices of electricity and gas grids, i.e. $EG_{cap}(t)$, $GG_{cap}(t)$, $SP(t)$ and $GP(t)$, respectively.

2. Set initial Lagrangian multipliers $\lambda^{r=0}(t)$, $\mu^{r=0}(t)$ and $\alpha^{r=0}(t)$.

3. **Optimization.** Given $\lambda^r(t)$, $\mu^r(t)$ and $\alpha^r(t)$, each prosumer solves the optimization problem presented in section 3.2.4 subject to the prediction models of the constraints in section 3.2.2.

   If the number of the current iteration (r) is even, use for the optimization an estimated $\lambda^r(t)$ (in our case, this is done by using the last obtained lambda). Else, use the lambda sent by the operator.

   Initial conditions
   $\hat{z}_{h,i}(1) = z_{h,i}(t)$
   $\hat{z}_{g,i}(1) = z_{g,i}(t)$

4. **Operators update** Lagrangian multipliers with the step size defined in section 3.2.4.
   If the number of the current iteration (r) is odd, use estimated values for $q_i(t)$ and $g_i(t)$ (in our case, this is done by using the last received values). Else, use the values given by prosumers.

$$\begin{aligned}
\lambda^{r+1}(t) &= \lambda^r(t) + \gamma_i^r(t)\left(\sum_{i=1}^{n}(q_i^r(t)*+g_i^r(t)*-B(t)\right)\\
\mu^{r+1}(t) &= \mu^r(t) + \varepsilon_i^r(t)\left(\sum_{i=1}^{n}(P_{prod,i}^r(t)-P_{d,i}(t))-EG_{cap}(t)\right)\\
\alpha^{r+1}(t) &= \alpha^r(t) + \beta_i^r(t)\left(\sum_{i=1}^{n} g_i^r(t) - GG_{cap}(t)\right)
\end{aligned}$$

   * shows the values that may have to be estimated.

5. If $\lambda_i^{r+1} - \lambda_i^r <= \delta$ and $\mu_i^{r+1} - \mu_i^r <= \delta$ and $\alpha_i^{r+1} - \alpha_i^r <= \delta$, and all the coupling constraints are met, go to next step. Else, go to step 3.

6. **Implementation** by the prosumers of the first of the computed sequence of control actions (thus applying receding horizon principle).
   $H_{prod,i}(t+1) = \hat{H}_{prod,i}(1)$
   $H_{aux,i}(t+1) = \hat{H}_{aux,i}(1)$
   $u_i(t+1) = \hat{u}_i(1)$
   $g_i(t+1) = \hat{g}_i(1)$

7. **Calculation** by the prosumer of the state variables at the time step $t = 1$ and $P_{prod,i}(t)$.

$$P_{prod,i}(1) = \frac{\eta_{p,i}}{\eta_{h,i}} \cdot \hat{H}_{prod,i}(1)$$
$$z_{h,i}(2) = z_{h,i}(1) + \hat{H}_{prod,i}(1) + \hat{H}_{aux,i}(1) - H_{d,i}(1)$$
$$z_{g,i}(2) = z_{g,i}(1) + \hat{u}_i(1)\ q_i(1) = \frac{\hat{H}_{prod,i}(1)}{\eta_h} + \frac{\hat{H}_{aux,i}(1)}{\eta_h} + \hat{u}_i(1)$$

8. **Restart** from step 1 with the next time-step.

Chapter 4

Simulation

In this chapter the simulations run to test the models and obtain results are explained. First, the implementation is exposed, followed by the setup of the simulations. Then, the performance indicators are described followed by the expectations on the results of every experiment. Finally, the results are given.

4.1 Implementation

4.1.1 Software

The algorithms used for the simulation are written in programming language Matlab, 2014b. This code makes use of open-source libraries and an additional optimization package. The optimization software used is the free academic licensed Gurobi. Gurobi optimization is a solver widely used for solving different kinds of programming, such as quadratic programming (QP), quadratically constrained programming (QCP) or mixed-integer linear programming (MILP), among others [57]. Another software used in this research is YALMIP, which serves as an interface between Matlab and the Gurobi Optimizer. YALMIP allows the previously stated problems to be stated in a clear and understandable manner and converts these formulations in such a way that the optimizer is used efficiently.

4.1.2 Hardware

The hardware used for running the simulations is an i5-3210m dual core processor with 8 GB RAM running on windows 8.1 64 bit.

4.1.3 Simulation code

To run the simulations, three different programs have been written: 1) A centralized algorithm, 2) a (partially) distributed algorithm and 3) an asynchronous distributed algorithm. The algorithms are delivered on the CD that comes with this thesis. All programs make use of the same set-up file, 'setup.m', in which all set-up and input

variables can be adapted, ranging from number of units to all predictions.

In the centralized algorithm, the controller makes the decisions for all prosumers and operators. The simulation is written in such a way that the controller has all information for all the prosumers and operators. The simulation can be run by executing the file 'maincode-centralized.m' in Matlab, which will use also the 'setup.m' and the 'createcontroller.m'. All needed data and files can be found in the folder 'MPC Centralized'.

In the distributed algorithm, each prosumer has its own controller and is able to optimize its own optimization problem, which results in computational advantages. However, they still need to exchange information with the different operators (Lagrangian multipliers). The distributed algorithm can be implemented in the same framework as the centralized model, in the sense that all information is treated in the same program again. In this case, the file 'createcontroller-dist.m' makes the function of the optimization in each prosumer, while the file 'maincode-distributed.m' makes the function of the different operators and, in the asynchronous, some functions of the prosumers. All needed data and files can be found in the folder 'DMPC'.

As explained before, an asynchronous model is also studied. In this case, the optimization by the nodes is not done at the same time that the optimization done by the operators, and so, some information has to be estimated. This simulation can be run by executing the file 'maincode-asyn.m' which also uses the files 'setup.m' and 'createcontroller-dist.m'. All needed data and files can be found in the folder 'DMPC-asyn'

4.2 Simulation setup

4.2.1 Network

The structure of the network plays an important role in the simulation code we are building. n prosumers are connected to the same power grid, the same low pressure gas grid, and one biomass anaerobic digester. In the two following pictures (Figure 4.1 and Figure4.2), it can be seen that the information flow is different for the centralized and the distributed layouts.

In the centralized network, each prosumer provides information to the central controller on states, inputs and objective functions. Based on the information received, the central controller determines the optimal supply and consumption plan and distributes them to each agent.

In contrast with the centralized approach, in the distributed network the prosumers communicate the desired individual supply and consumption levels to each associated operator. There are actually, two levels of optimization: the lower refers to the optimization problem solved by the prosumers, and the higher refers to the update of

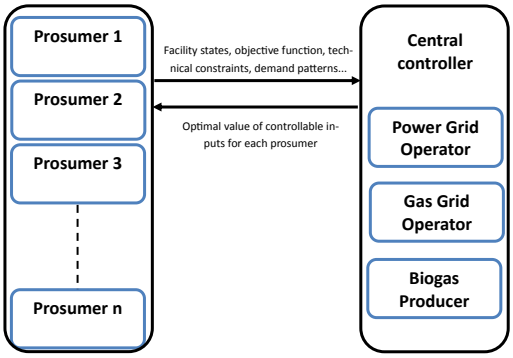

Figure 4.1: Centralized network settlement

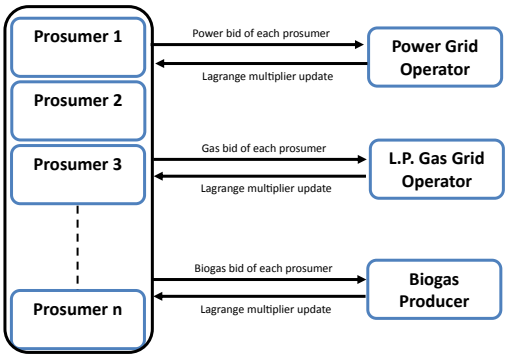

Figure 4.2: Distributed network settlement

shadow prices (Lagrangian multipliers) done by every operator.

4.2.2 Time resolution

The time resolution used in this research is basically based on the resolution of the data-sets. The power grid data and power demand have a resolution of 15 minutes, whereas the electricity price ($SP(t)$) and gas grid data sets are given hourly, and the gas prices are daily. All data is assumed to be constant during these time-steps. The amount of produced biogas by the anaerobic digester is basically constant.

4.2.3 Experiment

The simulations will be run with time of one day (96 periods), and a prediction horizon of an hour (4 periods). All the values of other variables are shown in Table 4.1.

Table 4.1: Values of the parameters of the objective function in the simulations

	Value	Source
c_{tp}	0,00001 €$/kWh^2$	[54]
c_{tg}	0,0001 €$/kWh^2$	[54]
c_g	0,003 €$/kWh$	[55]
C_{CHP}	0,002 €$/kWh$	[8]

The values of heat and power demand for the ten prosumers are shown in the Appendix as well the prices and the capacities of the low pressure gas grid and the power grid. The simulation is run in data of 21st of November of 2014, since it is the data that we had available. However, November demands in the Netherlands are normally similar to early months of spring demands, which makes this data relevant for two seasons of the year.

In this work, an efficiency of 85% will be used for the upgrader from biogas to green gas [42].

We assume that all prosumers have the same gas storage device, but may have diverse capacities around 1500 ft^3, which is to say 42,5 m^3. With the conversion of [51], it is to say, sizes of 4.25kWh.

As can be seen in [54], the price of the gas during 2012 was around 0.2 to 0.27 €/m^3, so in this work it is assumed to be 0.3€/m^3 because of the inflation tax during the period 2012-2015. The average price for the electricity at the spot market for the last few years has been of 50€/MWh.

Comparing SP(t) and GP(t), we see that nowadays, SP is always higher than GP, which will influence the result of the simulation. In some cases, they are forced to be the same, in order to see how the algorithms would behave.

At time-step k, each OS is initially associated with shadow prices(Lagrangian multiplier)of 0 or 0.0055, specified in each simulation results.

4.2.4 Scenarios

The performance of the control mechanism are evaluated based on the following scenarios:

- **Scenario 0: Centralized MPC and playing with values of the weighting factors w and y.** The only way to assess the value of these weighting factors is by forcing the sum of the biogas needs to be higher than the available biogas. This is because due to the assumption of $SP(t) > GP(t)$ done in this work, the prosumer will always prefer to use all the biogas in the prime mover, so it can sell excess electricity to the power grid.

- **Scenario 1: Centralized MPC with different configurations of prosumers**. Different setups of prosumers are simulated in this scenario, both with underloaded and overloaded capacity of the biogas producer.

- **Scenario 2: Synchronous dMPC with standard configuration**. In this scenario, all prosumers have the same characteristics. The goal of this scenario is to analyze how the Lagrangian multipliers (or shadow prices) behave.

- **Scenario 3: Asynchronous dMPC with standard configuration**. In this scenario all prosumers have the same characteristics. The goal of this scenario is to analyze if the Lagrangian multipliers behave in the same way than in the synchronous approach.

4.3 Performance indicators

The results of the different scenarios are evaluated in function of the performance measures discussed in this section.

1. The first performance index is the **estimated profit** that the prosumers get as a whole with the chosen prediction horizon. It is defined by:

$$\begin{aligned} Profit &= \sum_{t=0}^{t=T}\sum_{i=1}^{i=n}(SP(t)-Cchp)\cdot(P_{prod,i}(t)-P_{d,i}(t)) \\ &- c_{tp,i}\cdot(P_{prod,i}(t)-P_{d,i}(t))^2 \\ &+ (GP(t)-c_g)\cdot g_i(t) - c_{tg,i}\cdot g_i(t)^2 \\ &- w\cdot u_i(t)^2 - y\cdot H_{aux,i}(t)^2 \end{aligned} \tag{4.1}$$

   The profit can be interpreted as an economic profit but it does not correspond to the units of €since the data of the heat and power demand is in kW instead of kWh and it does not, therefore, fit the units of electricity grid price. However, it is chosen to use it since it is still comparable one case from the other, and gives some reference from the economic perspective.

2. The second performance index is the **time of the simulation**.

3. The third performance index is the **number of iterations** needed to converge to the optimum. It is only studied in the distributed models.

4. The fourth performance index is the **resources** needed with and without a μ-CHP. In order to calculate the resources used to generate the imported power from external parties, an efficiency of 45% is assumed [8].

5. The last performance assessment is the behavior of the Lagrangian multipliers, with respect to the underloaded or overloaded grid.

4.4 Expectations

The expectations of the model performance are elaborated here. They will be validated in Section 4.5.

4.4.1 Centralized vs distributed

With $n = 10$, it may be hard to see the difference, but it is supposed to be faster to converge to the optimum for the centralized, so the computational time should be smaller in the centralized than in the distributed approaches. The optimal profit should be equal in both cases, since there is no duality gap because of the convexity of the problem and constraints.

4.4.2 Centralized scenarios

In the simulations for centralized scenarios we play with different parameters.

1. All prosumers with or without prime mover: It is expected that the profit is higher in the case of having a primer mover, since prosumers have more flexibility in the way of fulfilling the local power demand and they can also sell excess electricity.

2. Overloaded and underloaded biogas capacity: It is expected that the maximum profit is higher in underloaded capacity. This is so because when $SP \geq GP$ and $SP \geq C_{CHP}$, the prosumer will want to produce as much electricity as possible, thus using as much biogas as possible, until the point where the costs are higher than the profit (i.e. as the transmission losses are quadratic, at some point they will be higher than profit, which is linear). Until this point, if a source is limited (e.g. biogas), the optimum will be lower than in the unlimited case.

3. Different sizes of heat storage (hot water tank): It is expected that the profit increases with higher size of storage, due to the fact that as long as the selling price of the electricity, $SP(t)$, is higher than the operational cost of the μ-CHP and than the selling price in the low pressure gas grid, $GP(t)$, the prosumer will try to produce as much energy as possible in the prime mover, thing that will be limited by the electricity grid capacity and by the heat storage size. However, this increasing in the profit is expected to only last until a maximum point where the bottleneck will no longer be the heat storage size, but another parameter, such as

the biogas availability or the electricity grid capacity. The expectations are based on the case where there is no cost for storing heat (assumed in our case).

4.4.3 Lagrangian multipliers

As explained before, the Lagrangian multipliers are set to start their iterations at value of zero or 0.005 depending on what we want to see. If the grid is overloaded (or the capacity of the biogas generator exceeded) it is expected that the Lagrangian multipliers will increase, thus forcing prosumers to reduce their bids. If, otherwise, the grid is underloaded (or capacity not reached) it is expected that the Lagrangian multiplier is decreased, with a minimum value of 0.

4.4.4 Distributed Synchronous vs Distributed Asynchronous

It is expected that in the asynchronous it takes more iterations then in the synchronous to converge to the optimal since it may not be any new updated information at every time step. The Lagrangian behaviour is expected to be similar for both cases.

4.5 Results

4.5.1 Values of the weighting factors w and y

When talking about the factor w, we aim to weight the cost of interacting with the biogas storage, either adding biogas or taking it from the storage. This factor is important because it will, when well adjusted, prevent the program to store and take gas from the storage constantly. It represents the cost of doing so, but we cannot find a way to assign a number to it, so we decide to run some simulations and assess the impact. The simulations are run for number of prosumers $n = 10$, during a day, 21st of November of 2014, ($T = 96$ periods) and with a prediction of horizon of one hour (4 periods). In order to make the value of the weighting factor meaningful, we decide to make the simulation with a diminished production of biogas, where it is needed to use the storage of gas ($u_i(t)$). Table 4.2 shows the results obtained in the simulations.

As can be seen, the weighting factor chosen does not turn into a change in profit. Therefore, the value with the minimum value for the computational time is chosen, i.e. $w = 0,05$. Recall that profit is a monetary value, but in not corresponding to €in these simulations.

In the case of the factor y, it weights the value of the heat produced by the auxiliary burner and is used to avoid starting and stopping it. Again, we cannot assign it a numerical value, so we ran the simulation with different values to see the impact. The simulations are run with a number of prosumers $n = 10$, during the same day, 21st of November of 2014, ($T = 96$ periods) and with a prediction of horizon of one hour (4 periods). In order to make the use of auxiliary burner necessary, we needed high heat

Table 4.2: Simulation results with different values of w.

w (€/kWh^2)	y(€/kWh^2)	Profit	comp. T (s)
0,05	0,5	25,79	162,543
0,0005	0,5	25,79	198,550
0,00001	0,5	25,79	165,225
5	0,5	25,79	169,908
50	0,5	25,79	166,715

demand and (almost) empty hot water tank, so we multiplied the value of the previous heat demand data by ten. The results are shown in Table 4.3

Table 4.3: Simulation results with different values of y.

w (€/kWh^2)	y (€/kWh^2)	Profit	comp. T (s)
0,5	0,5	-18.966,00	179,402
0,5	0,05	-1.771,40	207,306
0,5	0,0005	125,67	167,765
0,5	0,00001	143,88	187,186
0,5	0,000001	144,21	168,592
0,5	0,0000001	150,96	163,726
0,5	0,00000001	150,96	171,656

When looking at the results obtained with experimentation of y, the profit changes a lot depending on the value chosen. It can also be seen in Table 4.3 that when the value of y is small enough, the value of profit stabilizes. Therefore, the chosen value for the weighting factor y is 0,0000001, because it provides the lowest computational time.

4.5.2 Centralized simulations

All simulations are run with a number of prosumers $n = 10$, during the 21st of November ($T = 96$ periods) and with a prediction of horizon of one hour (4 periods). All cases are simulated with underloaded capacity (biogas available = 350kWh/15min) and overloaded capacity (biogas available = 40kWh/15min).

- Case without any μ-CHP: all prosumers have a boiler (efficiency 100%) and heat storage, but they cannot use the primer mover. Results are shown in Table 4.4.
- Standard configuration (SC): all prosumers with μ-CHP and gas and heat storage of similar sizes for all prosumers. Results are shown in Table 4.4.
- Different sizes of heat storage: all prosumers have with μ-CHP and gas and heat storage of similar sizes for all prosumers. It is experimented with three different sizes of heat storage (water tank). The sizes chosen are: S (100 liters),

M (150 liters), L (200 liters) and XL(300 liters). M is the size used for all other configurations. The results can be found in Table 4.5.

Table 4.4: Simulation results for the cases with no μ-CHP and Standard configuration.

		Total Profit	Comp. time (s)	Resources (kWh)
NO micro-CHP	Underl. (B=350)	-7,508	213,41	2462,7
	Overl. (B=40)	-7,508	199,50	
SC	Underl. (B=350)	237,27	174,09	2166,37
	Overl. (B=40)	33,09	196,48	

Comparing the cases with no μ-CHP installed and the standard configuration (see Table 4.4), it is clear that the profit is higher in the case with μ-CHP, which is expected, since in the scenario where $SP(t) >> C_{CHP}$, is more profitable for the prosumer to sell electricity instead of buying it. In the case of no prime movers used (no μ-CHP) the profit is negative since each prosumer has to spend money buying the electricity from the grid to fulfill its own demand.

We can also see that the computation time is a little higher in the case with prime movers installed, which makes sense because the calculation is also larger due to the calculation of the optimal values for the supply and consumption plan. It can also be seen that the implementation of the system saves 11% of the resources needed when importing the power from external sources. However, this calculation does not take into account the efficiency of the anaerobic digester, because it is calculated only the biogas needed for the production.

Table 4.5: Simulation results for the different sizes of heat storage.

		Total Profit	Computational time (s)
Underloaded (B=350)	Small	166,23	180,16
	Medium	237,27	174,09
	Large	308,23	192,99
	XL	364,16	175,76
Overloaded (B=40)	Small	32,98	172,37
	Medium	33,02	196,48
	Large	33,09	170,46
	XL	33,14	192,16

When comparing the results of different sizes of water storage, the results are as expected. In both cases, the profit grows with the size of the storage, because of the assumption of no costs for storage. The simulation is not run with a water tank bigger than 300 liters, as it is shown in [7] that the water tanks have a capacity from 100 to 200 liters [7]. Once the storage is big enough, the limiting resource is the biogas.

We also wanted to simulate the results with different sizes of gas storage, but in this simulation we have seen that it does not affect the profit, due to the length of a simulation (one day, which leaves no room for long-term storage prevision) and the length of the prediction horizon (one hour, which leaves no room for mid-term storage prevision). As the stored biogas can only be used for production (it is not allowed to store to sell in a better moment), the fact that the selling price of electricity is higher than the selling price for the gas should not affect the result.

In order to be able to see whether the use of model predictive control was a good choice, some simulations are run with different prediction horizons: H=1 (no predictions), H=4 (predictions of the next hour) and H=10 (predictions of the next 2 hours and a half). The results are shown in Table 4.6.

Table 4.6: Simulation with different prediction horizons.

	Total Profit	Computational time(s)
H=1	356,32	44,47
H=4	371,12	164,57
H=10	372,40	734,18

As can be seen in Table 4.6, the profit is really increased when predictions are used. This is due to the ability of the prosumers to adapt to what is coming in the upcoming future. The difference between being able to predict one hour (H=4) or two hours and a half (H=10) is not that big, since the demands, and selling prices of gas and electricity are quite constant. The computational time is increased as the predictive horizon increases.

4.5.3 Behavior of storage devices

Since the price of the electricity is higher than the price of the gas, each prosumer will try to produce as much electricity as possible in total. If the biogas is not a limiting factor, then the prosumer will try to produce as much electricity as possible, which is to say that will fulfill the heat storage device. Once the device is full, the only room for production on the next time steps will be the local heat demand, which will be taken from the water storage, thus leaving some room for production.

In the case of gas storage device, in the simulations run it is hardly used. This may be due to the fact that we are simulating in a simulation time of one day, which leaves

the long-period storage out of the simulation.

4.5.4 Distributed simulations: Studying the behavior of Lagrangian multipliers.

All simulations are run with number of prosumers $n = 10$, during half an hour ($T = 2$ periods) and with a prediction of horizon of one hour (4 periods) to analyze the behavior of the Lagrangian multipliers, which change their value within the internal iterations in the same time step. Therefore, we can just simulate for a fewer number of time steps. The simulations are based in five cases, which are:

- **Case 1**: Underloaded case with electricity selling price higher than gas selling price. Initial values for the Lagrangian multipliers are set to 0.005 to see, in this case, how they decrease. Hence, we need a value small enough so it does not make the optimization problem infeasible.
- **Case 2**: Underloaded case with electricity selling price equals to gas selling price. We choose to do this simulation because we know that the value of the Lagrangian multipliers are not independent, so λ may be affected by α and/or μ. As in the Case 1, the initial values for the Lagrangian multipliers are set to 0.005.
- **Cases 3 to 5**: Overloaded grids. In each of these cases we overload one and only one of the grids, so we get to see how the Lagrangian multipliers behave in these cases and how they affect each other. Whichever the grid is overloaded, its Lagrangian multiplier is set to an initial value of 0, because we expect it to increase and it is more visible when starting from 0.

In Table 4.7 there is the comparable data between cases. We can see that the profit is the same that the one in the centralized, which makes sense, because of the convexity of the problem. The computational time is also as expected, i.e. lower than in centralized, because the computational load of a distributed model is usually lower. When equalizing the selling price of the gas with the selling price of electricity, the profit increases, because selling the gas becomes an interesting option as well. This interest in making $g_i(t)$ higher also increases the number of iterations needed of α, the Lagrangian multiplier associated to the amount of gas to be sold ($g_i(t)$).

We can also see in Table 4.7 that when any of the grids is overloaded, the profit is reduced. A curious case to comment is that when the gas grid is overloaded it also affects in the iterations of the other two. This is because of the relation on their coefficients. α is associated with the amount of the gas to be sold to the grid $g_i(t)$, which is also inside the constraint of λ. And at the same time, the contraint of μ is associated to the power production $P_{prod,i}(t)$ which is coupled to the heat production by the prime mover $H_{prod,i}(t)$, also inside the constraint of λ. We will see this further in Figure 4.9.

We can see in Figure 4.3, the behavior of the Lagrangian multipliers (λ, μ and α) in the underloaded case 1. The value of the Lagrangian multiplier decreases as the

Table 4.7: Simulation results for the 5 cases of the distributed model with a = 0,005

				Initial value			Iterations		
		Profit	Comp. t(s)	λ	μ	α	λ	μ	α
Underl.	SP > GP	1,27	3,89	a	a	a	9	2	2
	SP =GP	9,34	27,91	a	a	a	9	2	3
Overl.	B = 40	0,51	3,00	0	a	a	4	2	2
	C. EG = 25	1,23	32,18	a	0	a	3	3	2
	C. GG= 600	9,06	38,46	a	a	0	121	78	83

iterations move on.

We can see in Figure 4.4, the behavior of the Lagrangian multipliers (λ, μ and α) in the underloaded case 2. As in the case 1, the value of the Lagrangian multiplier decreases as the iterations move on.

In Figure 4.5, the results of the case 3 are shown. In this case it is assumed that the maximum biogas available, $B(t)$, is limited ($B = 40$). λ is the Lagrangian multiplier associated to the biogas availability and it can be seen that it has changed from the previous cases. In this case the value of λ is initiated at 0.

In Figure 4.6 the behavior of this Lagrangian multiplier is compared to the sum of the supply bids ($\sum_{i=1}^{n}\sum_{t=1}^{T} q_i(t) + g_i(t)$) that the operator receives from the prosumers. At the iteration 1, when $\lambda = 0$, we see that the consumption of biogas asked by the prosumers is higher than the available amount. Therefore, λ increases its value to the one in iteration 2. Then the prosumers react to this value and their sum of the supply bids is too low, so the Lagrangian multiplier is decreased by the operator. In this case, the sum of prosumers bids reaches the maximum, which is also the optimum.

In Figure 4.7, the results of the case 4 are shown. In this case it is assumed that the electricity grid capacity, $EG_{cap}(t)$, is limited ($EG_{cap}(t) = 25kWh$). μ is the Lagrangian multiplier associated to the capacity of the electricity grid and it can be seen that it has changed from the previous cases. In this case the value of μ is initiated at 0, in order to see better its behavior. In Figure 4.8 the behavior of this Lagrangian multiplier is compared to the sum of the supply bids ($\sum_{i=1}^{n}\sum_{t=1}^{T} P_{prod,i}(t) - P_{d,i}(t)$) that the operator receives from the prosumers. At the iteration 1, when $\mu = 0$, we see that the production of electricity proposed by the prosumers is higher than the current capacity of the grid. Therefore, μ is increased by the operator to the value in iteration 2. Then, when the prosumers react to this value, their sum of the supply bids is too low, so the Lagrangian multiplier is decreased by the operator. In this case, the sum of prosumers bids reaches the maximum, which is also the optimum.

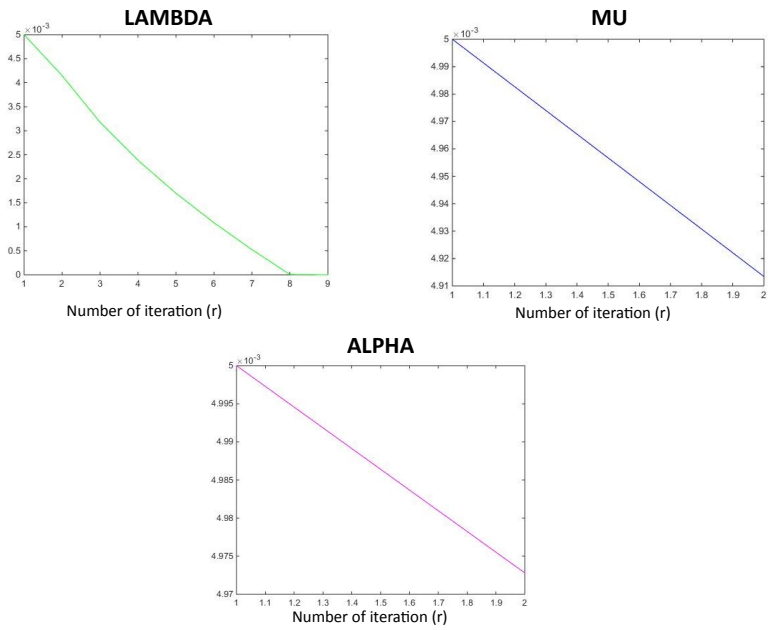

Figure 4.3: Evolution of the three Lagrangian multipliers in case 1, where the Lagrangian multipliers decrease from their initial value because there is no overloading.

In Figure 4.9, the results of the case 5 are shown. In this case it is assumed again that the selling prices for gas and for electricity are the same ($GP(t) = SP(t)$) and that the gas grid capacity, $GG_{cap}(t)$, is limited ($GG_{cap}(t) = 600kWh$). α is the Lagrangian multiplier associated to the capacity of the low pressure gas grid and it can be seen that it has changed from the previous cases. In this case the value of α is initiated at 0. In Figure 4.10 the behavior of this Lagrangian multiplier is compared to the sum of the supply bids ($\sum_{i=1}^{n}\sum_{t=1}^{T} g_i(t)$) that the operator receives from the prosumers. At the iteration 1, when $\alpha = 0$, we see that the production of electricity proposed by the prosumers is higher than the current capacity of the grid. Therefore, μ is increased by the operator to the value in iteration 2. Then, when the prosumers react to this value, their sum of the supply bids is too low, so the Lagrangian multiplier is decreased by the operator. In this case, the sum of prosumers bids reaches the maximum, which is also the optimum.

We can also see in case 5 how the Lagrangian multiplier of λ is affected by the limitation, and its behavior is very similar at α's behavior.

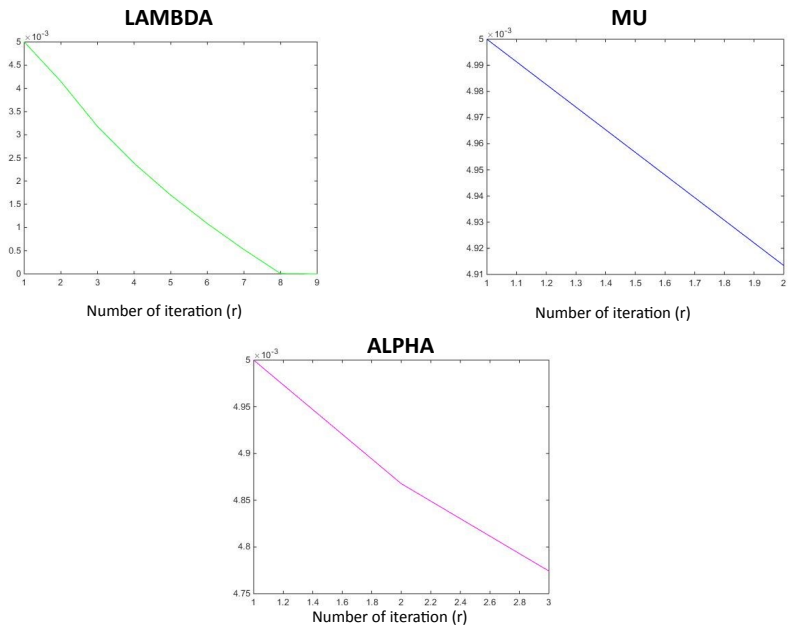

Figure 4.4: Evolution of the three Lagrangian multipliers in case 2, where they all decrease, but the number of iterations needed in α is higher than in case 1.

Simulations with different sizes for the step-size

In order to see how the coefficient that multiplies the step size affects the number of iterations, some simulations are done in the underloaded case. The results of such simulations can be seen in Table 4.8.

4.5.5 Asynchronous vs Synchronous

In Table 4.9 we compare the results of the synchronous and the asynchronous case. While the profit keeps the same value, the computational time increases in the asynchronous case due to the need of more iterations to have the same information about the biogas available. This is also seen in the number of iterations needed in each case for the Lagrangian multiplier λ. This fact is because the operator of the biogas producer receives information only once every two iterations, same frequency as the prosumer receives information from the operator.

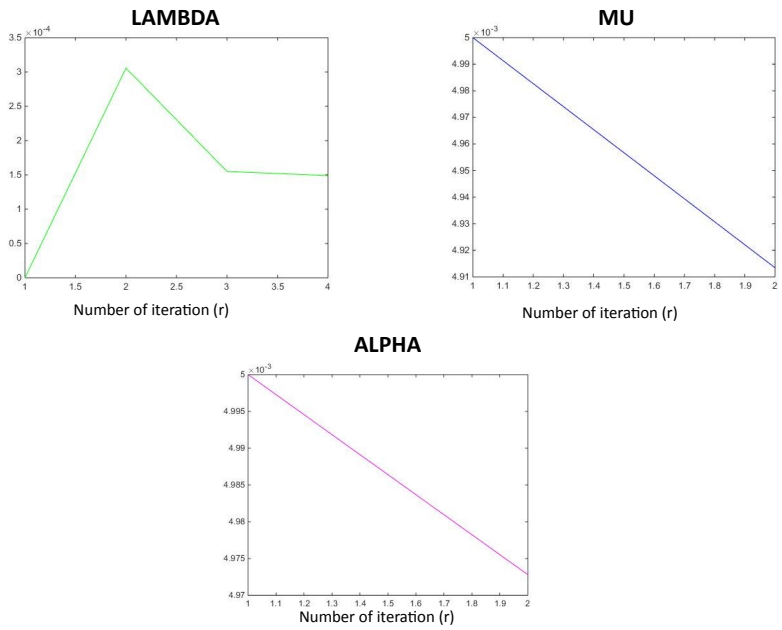

Figure 4.5: Evolution of the three Lagrangian multipliers in case 3, where μ and α only decrease while λ fluctuates.

Table 4.8: Results for different values of the coefficient of the step size.

N iterations					
coef	lambda	mu	alpha	t(s)	Profit
0,0055	3	3	3	3,2196	1,2797
0,00055	3	3	3	7,8184	1,2797
0,000055	3	16	9	8,2138	1,4668
0,0000055	8	70	175	28,9321	1,3259
0,00000055	258	2	3	41,8256	0,0013

Table 4.9: Results of the comparison of synchronous dMPC and asynchronous dMPC

			Initial value			Iterations		
	Profit	Comp.time (s)	lambda	mu	alpha	lambda	mu	alpha
Synch.	1,27	3,89	0,005	0,005	0,005	9	2	2
Asynch.	1,27	5,43	0,005	0,005	0,005	15	2	2

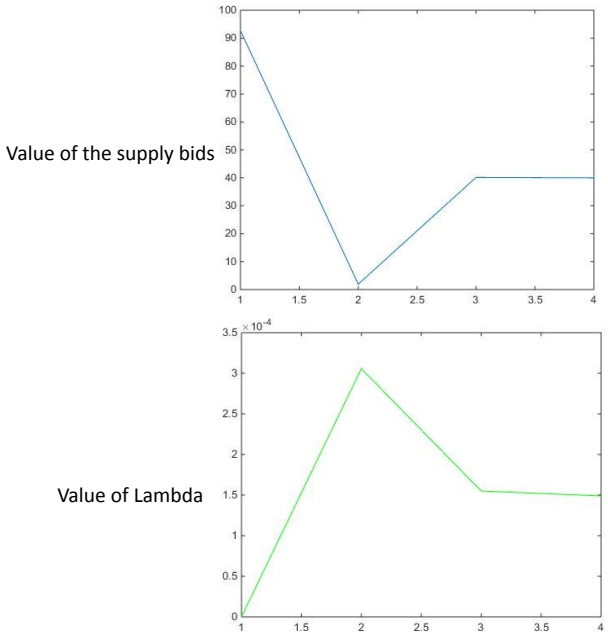

Figure 4.6: Evolution of λ and the sum of the supply bids in case 3

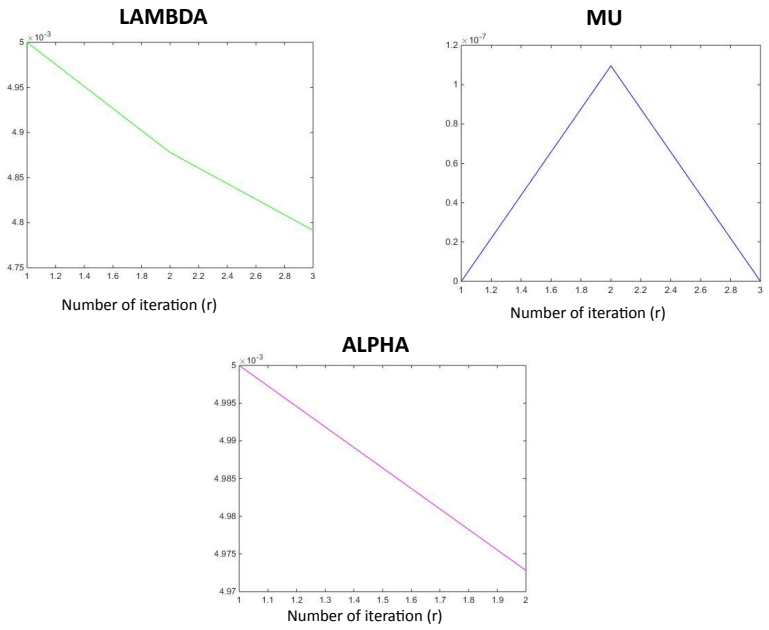

Figure 4.7: Evolution of the three Lagrangian multipliers in case 4, where λ and α only decrease while μ has a previous growth.

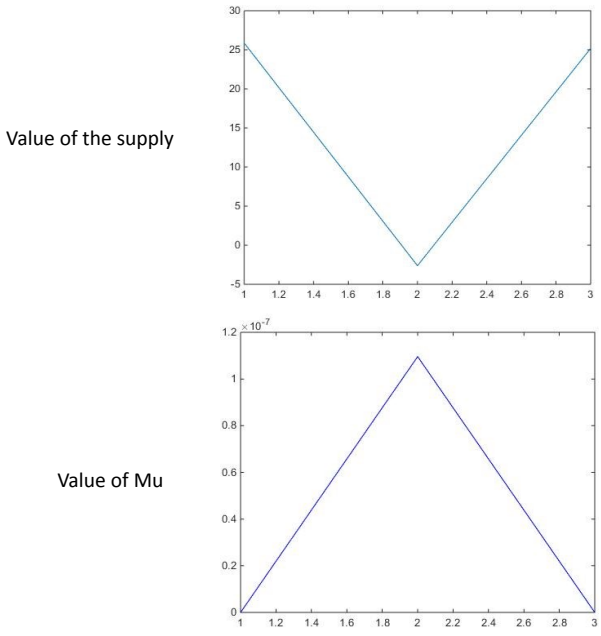

Figure 4.8: Evolution of μ and the sum of the supply bids in case 4

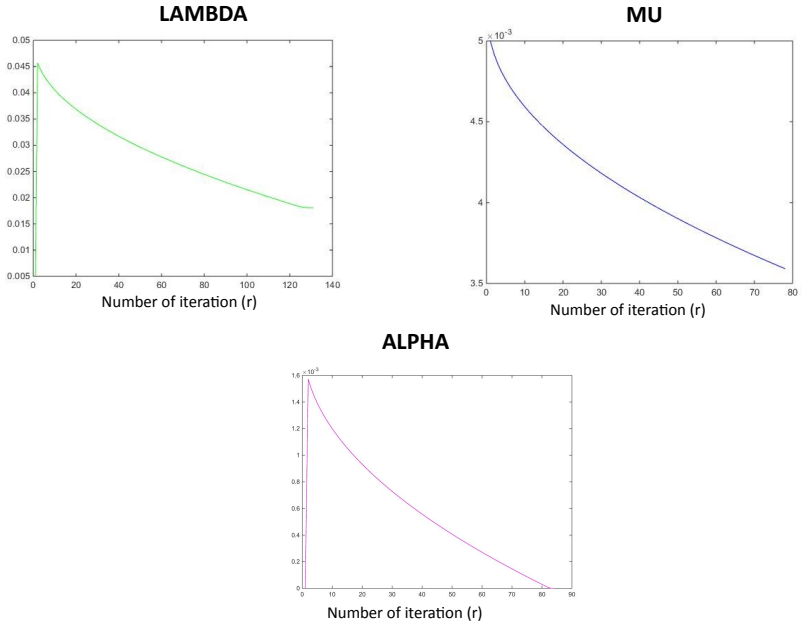

Figure 4.9: Evolution of the three Lagrangian multipliers in case 5, where μ only decreases, while λ and α increase in the first iterations and then decrease.

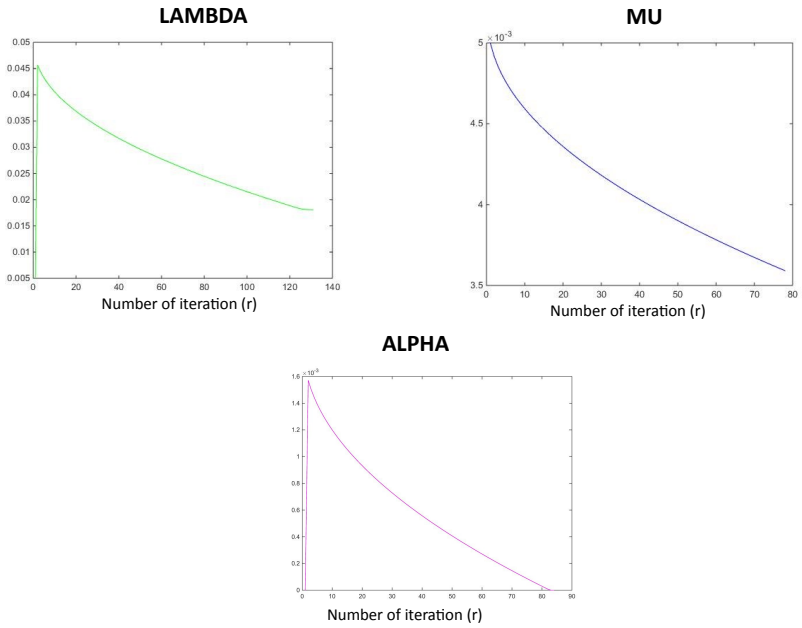

Figure 4.10: Evolution of α and the sum of the supply bids in case 5

Chapter 5

Discussion

5.1 Findings

In this work, three algorithms (cMPC, dMPC and dMPC asynchronous) are designed to control the consumption and supply of the micro grid presented in Chapter 2, by applying MPC framework on a network of prosumers. In the centralized control algorithm a centralized controller makes decisions upon all prosumers in the network, whereas in the distributed control algorithms (synchronous and asynchronous), each prosumer makes its own decisions upon its supply and consumption levels, by maximizing its profit. Dual decomposition combined with the projected sub-gradient method is applied to obtain the distributed model from the centralized model. Because of no duality gap, optimal values for the dual problem also optimize the original (primal) problem.

The performance of the algorithms is tested in simulations, where all algorithms produce feasible solutions. In the centralized, it can be seen that the performance is improved compared to the same scenario without power production, in terms of profit and resource savings. The saving in resources needed is of around 12% and the profit, used as an economical approach, is higher. In the centralized case it is also studied how the storage size affects the optimal value of the profit, resulting in the conclusion that the higher the storage, the higher the profit, in the case of not including storing costs.

It is proved that the MPC framework allows the prosumers to adapt to the predicted future, and therefore, the profit obtained using this method is higher.

We study the behavior of the Lagrangian multipliers in both, underloaded and overloaded grids. The results are as expected, i.e. reacting at prosumers supply and consumption bids by increasing or decreasing the value of the Lagrangian multiplier. When the grids and capacity are underloaded, the Lagrangian multipliers decrease until reaching the optimum. When, on the other hand, the grids are overloaded or the capacity is exceeded, the Lagrangian multipliers increase their value until the supply and consumption bids stay inside the limits. This is to say that the Lagrangian multipliers

perform their function as link of information between the prosumers and the operators of the grids and biogas producer.

In this work, the majority of the scenarios are built with the selling price of electricity being higher than the selling price for the gas, i.e. $SP(t) \geq GP(t)$. However, in the future, the selling price of the gas could be higher, then the results may be different.

In the literature review, MPC is compared with other control systems. Although qualitative arguments have been exposed about what makes MPC have advantages over other control mechanisms, no quantitative arguments can be given. Therefore, no conclusions can be taken about the performance of the developed algorithm compared to other methods.

5.2 Remarks and possible improvements

The expectations for the different simulations have been explained in Chapter 4. The results of all simulations shown in Chapter 4 are according to the expectations. However, the results presented in Section 4.5 are based on one specific simulation set-up. Due to time restrictions, no larger number of simulations could be performed. Therefore, a major drawback of the run simulations is that their results cannot be validated statistically. In addition, it would be better to have a simulation of the whole year to see how the system behaves in case of high heat demand (winter) and low heat demand (summer). Because of limited time and data available, the simulation times are set to a day and an hour but the results would be more significant if the simulation time was higher. This way, the behavior of energy storage devices on long term could be studied and optimized.

The distributed model has a longer computational time compared to the centralized. An improvement that can be done in future research is to use another method of subgradient iteration for updating the Lagrangian multipliers, like the accelerated gradient method [53].

Additionally, another point of the simulation that can be improved is making the performance indicator *profit* have a monetary unit. This could be done by just adjusting all data introduced in the algorithm to have the same units.

Another drawback of simulation setup is that the asynchronous method could be faster and this is due, most probably, to the fact that the prosumer and the operator never receive the response at the same moment that they are iterating. This is due to the simplification used in the asynchronous algorithm, where this approach is chosen in order to simplify the algorithm. In future work it may be interesting to study an asynchronous model with different clock discordance, random for example.

Also, in the asynchronous, the estimation on lambda and the supply bids is exactly the last received one. If the estimation was more precise, based on patterns (e.g. of the very specific prosumer) and previous performances for example, probably the com-

putational load and time of the asynchronous algorithm would be better. This is once again due to the simplification done in this work.

5.3 Future research

This research is subject to research boundaries and simplifications. To achieve more accurate models, some of the boundaries and simplifications can be studied further as part of future research. The most important fields for future research are discussed below.

1. The predictions are not included in this model as it is assumed that each operator does the predictions according to historical data. In the simulations, the prediction used is the real data for these time steps. It could be valuable to combine MPC (and dMPC) with a prediction algorithm and then assess this prediction and how the model behaves in this case.

2. The costs of buying all the devices are not studied in this work, so it may be interesting to do an economic study of this case, in which the prosumers are able to fulfill their local demands basically with their own agricultural wastes, and in most of cases, even obtaining revenue. The payback period can be studied there.

3. Nowadays, when efficient electric batteries are becoming a reality, it can be interesting to study the case with also electric power storage. In this way, the house can be absolutely independent from the grid.

Bibliography

[1] Farhad S., Hamdullahpur F. and Yoo, Y. Performance evaluation of different configurations of biogas-fuelled SOFC micro-CHP systems for residential applications. *International journal of hydrogen energy* vol. 35 (8) pp. 3758-3768, 2010.

[2] Van der Veen R.A.C. and De Vries L.J. Balancing market design for a decentralized electricity system: Case of the Netherlands. *Infrastructure Systems and Services: Building Networks for a Brighter Future (INFRA), 2008 First International Conference on* pp. 1-6, 2008.

[3] Staffell I. and Green R. The cost of domestic fuel cell micro-CHP systems *International Journal of hydrogen energy* vol. 38(2), pp.1088-1102, 2013.

[4] Howing M. Smart Heat and Power, utilizing the flexibility of micro generation. *Proceedings IEEE* vol. 99(1), pp.200-213, 2010.

[5] Power Matching City. $http://www.powermatchingcity.nl/site/pagina.php?id=$ 46, accessed on July 2015.

[6] Napoli R., Gandiglio M., Lanzini A. and Santarelli M. Techno-economic analysis of PEMFC and SOFC micro-CHP fuel cell systems for the residential sector *Energy and Buildings* vol.113, pp. 131-146, 2015.

[7] Houwing M., Negenborn R.R. and De Schutter B. Demand Response With Micro-CHP Systems *Proceedings of the IEEE* , Vol. 99(1), pp. 200-213, 2011.

[8] Larsen G.K.H., van Foreest N.D. and Scherpen J.M.A. Distributed MPC Applied to a Network of Households With Micro-CHP and Heat Storage. *IEEE Transactions on a Smart Grid*, vol. 5(4), pp. 2106-2114, 2014.

[9] Yanmar Yanmar biogas fuelled CP. $https://www.yanmar.com/global/energy/bio_gas_micro_cogeneration_package/$ accessed on August 2015.

[10] Bakker J. The effect of different control methods on a small network of micro-chp's. *Control related to usage levels, requirements and technologies* Master thesis, RUG, 2008.

[11] Kok J.K., Warmer C.J. and Kamphuis I.G. Multiagent control in the electricity infrastructure *Proceedings of the International Conference on Autonomous Agents* pp. 115-122, 2005.

[12] Doornbos E. Distributed control and prince mechanisms for a small network of micro-chps. Master Thesis, RUG, 2010.

[13] Rantzer A. On prize mechanisms in linear quadratic team theory. *46th IEEE conference on Decision and Control* pp. 1112-1116, New Orleans, LA, Dec.2007.

[14] Napoli R, Gandiglio M., Lanzini A. and Santarelli M. Techno-economic analysis of PEMFC and SOFC micro-CHP fuel cell systems for the residential sector *Energy and Buildings* vol.103 pp.131-146, 2015.

[15] Alkano D., Nefkens W.J., Scherpen J.M.A, Volkerts M. Optimal Flow Control in a Micro Grid of Biogas Prosumers Using Model Predictive Control *The 21th International Symposium on Mathematical Theory of Networks and Systems*, pp.592-598, 2014

[16] Larsen G.H.K. Distributed control in a network of households with microchp *University of Groningen* 2011

[17] Giselsson P. and Rantzer A. Distributed model predictive control with suboptimality and stability guarantees. *IEEE Conference on Decision and Control, Atlanta, Georgia, USA*, 2010.

[18] Tjalkens T. and Willems F. Convexity and optimization *Technische universiteit Eindhoven* 2007. Available at $http://www.sps.ele.tue.nl/members/T.J.Tjalkens/5jk00/dictaat/06/convexity-article.pdf$.

[19] Vandenberghe L. and Boyd S. Convex Optimization. *Cambridge University Press,* 2009.

[20] Boyd S. and Mutapcic A. Subgradient methods *Lecture notes of EE364b, Stanford University, Winter Quarter* 2006.

[21] Roth E., Verhoef L. and Dingenouts M. Concerted action for offshore wind energy deployment (COD), 2004.

[22] Celador A., Campos and Odriozola M. and Sala J.M. Implications of the modelling of stratified hot water storage tanks in the simulation of CHP plants. *Energy Conversion and Management*, vol.52 (8), pp. 3018-3026, 2011.

[23] Fang X., Misra S., Xue, G. and Yang, D. Smart Grid - The New and Improved Power Grid: A Survey. *Communications Surveys & Tutorials, IEEE*, vol.14 (4), pp. 944-980, 2012.

[24] Fang X., Xue, G. and Yang, D. Online strategizing distributed renewable energy resource access in islanded microgrids. *IEEE Global Telecommunications Conference (GLOBECOM 2011)*, 2011.

[25] Mohsenian-Rad A., Wong V., Jatskevich, J., Schober R. and Leon-Garcia, A. Autonomous demand-side management based on game-theoretic energy consumption scheduling for the future smart grid. *IEEE Transactions on Smart Grid*, vol.1 (3), pp. 65-72, 2010.

[26] Mhagheghi S., Stoupis J., Wang Z., Li Z. and Kazemzadeh H. Demand Response architecture: integration into the distribution management system. *IEEE SmartGridComm*, pp. 501-506, 2010.

[27] Ziebolz H. and Paynter H. M. Possibilities of a two-time scale computing system for control and simulation of dynamic systems. *Proc Natl Electronics Conf.*, vol. 9, 1954.

[28] Rantzer, A. Dynamic dual decomposition for distributed control *IEEE American Control Conference*, pp. 884-888, 2009.

[29] Gunaseelan, V. N. Anaerobic digestion of biomass for methane production: a review. *Biomass and bioenergy*, vol. 13(1) pp. 83-114, 1997.

[30] Weiland, P. Biomass digestion in agriculture: a successful pathway for the energy production and waste treatment in Germany *Engineering in Life Sciences*, vol. 6(3) pp. 302-309, 2006.

[31] CME Group Seasonality and Storage in Natural Gas - Resource guide *Energy Products, Paradigm* http://www.cmegroup.com/trading/energy/seasonality-and-storage-in-natural-gas.html, 2011, accessed in July 2015.

[32] Krich K., Augenstein D., Batmale J.P., Benemann J., Rutledge B., Salour D. Biomethane from Dairy Waste: A Sourcebook for the Production and Use of Renewable Natural Gas in California *American Biogas council* 2005.

[33] PWC Inventarisatie van verschillende afzetroutes voor groen gas *Agentschap NL. Ministerie van Economische Zaken, Landbouw en Innovatie* 2012.

[34] Hamada Y. and Nakamura M. Field performance of a polymer electrolyte fuel cell for a residential energy system. *Renewable Sustainable Energy Rev.*, vol.9 (4) pp. 345-362, 2005.

[35] Kallitsis M.G., Michailidis G., Devetsikiotis M. A framework for optimizing measurement-based power distribution under communication network constraints. *IEEE SmartGridComm10.*, pp. 185-190, 2010.

[36] Anderson R.N., Boulanger A., Powell W.B. and Scott W. Adaptive stochastic control for the smart grid. *Proceedings of the IEEE.*, vol.99 (6) pp. 1098-1115, 2011.

[37] Clement-Nyns, Haesen E. and Driesen J. The impact of charging of multiple plug-in hybrid electric vehicles on a residential distribution grid. *IEEE Transactions on Power Systems*, vol.25 pp. 371-380, 2010.

[38] Conejo A.J., Morales J.M. and Baringo L. Real-time demand response model *IEEE Transactions on Smart Grid*, vol.1 (3) pp. 236-242, 2010.

[39] Hutson C., Venayagamoorthy G.K. and Corzine K.A. Intelligent scheduling of hybrid and electric vehicle storage capacity in a parking lot for profit maximization in grid power transactions. *IEEE Energy 2030.*, pp. 1-8, 2008.

[40] Mylopoulos, J. Conceptual modelling and Telos 1 *Citeseer* 2008.

[41] Van den Boom T.J.J and Stoorvogel A.A. Model Predictive Control, lecture notes *DISC* 2010.

[42] Bekkering J., Broekhuis A. A. and Van Gemert W. J. T. Optimisation of a green gas supply chain A review. *Bioresource technology*, vol.101 (2) pp. 450-456, 2010.

[43] dAccadia M.D., Sasso M., Sibilio S. and Vanoli L. Micro-combined heat and power in residential and light commercial applications. *Applied Thermal Engineering* vol.23 (10) pp. 1247-1259, 2003.

[44] Pehnt M., Cames M., Fischer C., Praetorius B., Schneider L., Schumacher K. and Vob J. Micro cogeneration: Towards Decentralized Energy Systems. *Springer-Verlag* Berlin, Germany, 2006.

[45] Beith R., Burdon I.P. and Knowles M. Micro Energy Systems: Review of Technology, Issues of Scale and Integration. *Professional Engineering Publishing* Suffolk, U.K. 2004.

[46] Chowdhury S., Yasir M., Uemura Y., Mohamed N.M., Uddin A., and Yanagida T. Application of Micro- or Small-Scale Biomass- Derived Fuel System for Power Generation. *Biomass and Bioenergy: Applications (chapter 17), Springer International Publishing* Switzerland, 2014.

[47] Dong L., Liu H. and Riffat S. Development of small-scale and micro-scale biomass-fuelled CHP systemsa literature review. *Applied Thermal Engineering* vol.29 (1112), pp. 21192126, 2009.

[48] Maghanki M.M., Ghobadian B., Najafi G. and Galogah R.J. Micro combined heat and power (MCHP) technologies and applications *Renewable and Sustainable Energy Reviews* vol.28, pp. 510-524, 2013.

[49] Hobbs B.F., Drayton G. and Fisher, E. Improved transmission representations in oligopolistic market models: quadratic losses, phase shifters, and DC lines *IEEE Transactions on Power Systems* vol. 23 (3), pp. 1018-1029, 2008.

[50] Wismer D.A. and Chattergy R. Introduction to nonlinear optimization: A problem solving approach. *North Holland Series in System Science and Engineering* New York, 1978.

[51] Eriksson O. Environmental technology assessment of natural gas compared to biogas *University of Gvle, Sweden* 2010. av. at: $http://cdn.intechopen.com/pdfs/11474/InTech-Environmental_technology_assessment_of_natural_gas_compared_to_biogas.pdf$

[52] Hu C., Luo S., Li Z., Wang X., and Sun, L. Energy Coordinative Optimization of Wind-Storage-Load Microgrids Based on Short-Term Prediction *Energies* vol.8 (2), pp. 1505-1528, 2015.

[53] Ji S. and Ye J. An accelerated gradient method for trace norm minimization. *Proceedings of the 26th annual international conference on machine learning.* ACM, 2009.

[54] Kuiper I. Model Predictive Control For cooperation of multiple PtG facilities Master thesis, RUG, 2014.

[55] Nefkens W.J. Distributed control of a micro gas grid of prosumers Master thesis, RUG, 2013.

[56] Pons J.L. Distributed Control of Electricity Demand - The application of distributed Model Predictive Control on a network of washing machines Master thesis, RUG, 2013.

[57] Gurobi. URL: *www.gurobi.com*

Appendices

Appendix A

Data used

Table A.1: Data on the selling price of gas ($GP(t)$), and electricity ($SP(t)$), and the capacities of both grids, electricity(EG) and gas (GG)

T-step	GP(t) (€/kWh)	SP(t)(€/kWh)	Capacity EG (t)(kWh)	Capacity GG(t)(kWh)
1	0,00625	0,0304	520,58458	791,0835125
2	0,00625	0,0304	520,58458	779,7110315
3	0,00625	0,0304	520,58458	771,892173
4	0,00625	0,0304	32,93426	767,2948611
5	0,00625	0,02886	619,1949448	765,58702
6	0,00625	0,02886	619,1949448	766,4365737
7	0,00625	0,02886	145,9448952	769,5114464
8	0,00625	0,02886	796,246802	774,4795621
9	0,00625	0,02805	412,8873278	781,008845
10	0,00625	0,02805	404,1455264	788,6241131
11	0,00625	0,02805	165,4254053	796,2777602
12	0,00625	0,02805	276,748472	802,7790741
13	0,00625	0,02518	542,2674689	806,9373425
14	0,00625	0,02518	576,1352825	808,0101488
15	0,00625	0,02518	492,1188241	807,0482584
16	0,00625	0,02518	55,70266838	805,5507326
17	0,00625	0,02446	55,70266838	805,0166325
18	0,00625	0,02446	502,2994065	806,7468267
19	0,00625	0,02446	219,6117875	811,2494139
20	0,00625	0,02446	473,655797	818,8343005
21	0,00625	0,02733	473,655797	829,8113925
22	0,00625	0,02733	212,3219879	844,0362673
23	0,00625	0,02733	212,3219879	859,5471864
24	0,00625	0,02733	212,3219879	873,9280823
25	0,00625	0,03492	139,2877451	884,7628875
26	0,00625	0,03492	4,695598791	890,5700215
27	0,00625	0,03492	165,7462705	893,6058519
28	0,00625	0,03492	39,81050693	897,0612332
29	0,00625	0,04647	120,4662016	904,12702
30	0,00625	0,04647	716,1225002	916,8343809
31	0,00625	0,04647	339,2472762	932,5757408
32	0,00625	0,04647	63,19738583	947,5838383
33	0,00625	0,04375	63,19738583	958,0914125
34	0,00625	0,04375	340,9949894	961,6513061
35	0,00625	0,04375	1008,880118	961,0967779
36	0,00625	0,04375	252,404916	960,5811907
37	0,00625	0,04994	214,8300082	964,2579075
38	0,00625	0,04994	469,1632146	974,7559813
39	0,00625	0,04994	504,9326508	988,6072268
40	0,00625	0,04994	280,1200976	1000,819149
41	0,00625	0,04372	491,1571919	1006,399253
42	0,00625	0,04372	366,7169595	1001,84865

Table A.2: Data on the selling price of gas ($GP(t)$), and electricity ($SP(t)$), and the capacities of both grids, electricity(EG) and gas (GG) (continuation of Table A.1)

T-step	GP(t) (€/kWh)	SP(t)(€/kWh)	Capacity EG (t)(kWh)	Capacity GG(t)(kWh)
43	0,00625	0,04372	366,7169595	989,6428844
44	0,00625	0,04372	509,0725593	973,7511051
45	0,00625	0,04401	288,1159227	958,1424625
46	0,00625	0,04401	627,9418631	946,0196274
47	0,00625	0,04401	463,5568902	937,5193548
48	0,00625	0,04401	806,173902	932,0119204
49	0,00625	0,04484	474,0847797	928,8676
50	0,00625	0,04484	594,5517299	927,2063721
51	0,00625	0,04484	789,9772513	925,1470258
52	0,00625	0,04484	670,8279144	920,5580528
53	0,00625	0,03999	306,4536555	911,307945
54	0,00625	0,03999	262,2462397	896,2715019
55	0,00625	0,03999	631,0022045	878,3487548
56	0,00625	0,03999	526,4092899	861,4460428
57	0,00625	0,0412	1002,123148	849,469705
58	0,00625	0,0412	773,8868034	845,088695
59	0,00625	0,0412	393,7567765	846,0224243
60	0,00625	0,0412	263,2799414	848,752919
61	0,00625	0,03994	405,3652422	849,762205
62	0,00625	0,03994	880,9486433	846,5390853
63	0,00625	0,03994	757,439985	840,5994705
64	0,00625	0,03994	1079,861005	834,4660479
65	0,00625	0,049	572,4773981	830,661505
66	0,00625	0,049	1371,752684	831,3736764
67	0,00625	0,049	436,8432364	837,4509859
68	0,00625	0,049	259,5568568	849,4070042
69	0,00625	0,03754	699,0065735	867,7553025
70	0,00625	0,03754	441,6818103	892,3560602
71	0,00625	0,03754	379,1079968	920,4558911
72	0,00625	0,03754	430,1168873	948,6480177
73	0,00625	0,04552	430,5244614	973,5256625
74	0,00625	0,04552	323,1099678	992,4378341
75	0,00625	0,04552	971,5056163	1005,756686
76	0,00625	0,04552	567,2963087	1014,610157
77	0,00625	0,04714	412,4196216	1020,126188
78	0,00625	0,04714	730,9135244	1023,210491
79	0,00625	0,04714	411,8589859	1023,879878
80	0,00625	0,04714	411,8589859	1021,928934
81	0,00625	0,04215	324,9891283	1017,152245
82	0,00625	0,04215	176,0113305	1009,643349
83	0,00625	0,04215	85,46663258	1000,691595
84	0,00625	0,04215	85,46663258	991,8852888

Table A.3: Data on the selling price of gas ($GP(t)$), and electricity ($SP(t)$), and the capacities of both grids, electricity(EG) and gas (GG) (continuation of Table A.2)

T-step	GP(t) (€/kWh)	SP(t)(€/kWh)	Capacity EG (t)(kWh)	Capacity GG(t)(kWh)
85	0,00625	0,04393	289,7973474	984,8127325
86	0,00625	0,04393	172,0297514	980,6378632
87	0,00625	0,04393	243,8573916	978,8271505
88	0,00625	0,04393	551,3931667	978,4226976
89	0,00625	0,04318	211,7021333	978,4666075
90	0,00625	0,04318	328,9730414	977,64701
91	0,00625	0,04318	780,2799918	973,2361425
92	0,00625	0,04318	538,7118306	962,1522694
93	0,00625	0,04146	790,6221223	941,313655
94	0,00625	0,04146	561,446654	909,2533535
95	0,00625	0,04146	876,404591	870,9635796
96	0,00625	0,04146	678,3946094	833,0513377
97	0,0075	0,0304	844,8050405	802,1236325
98	0,0075	0,0304	712,4841377	783,1407889
99	0,0075	0,0304	202,0990825	774,4764138
100	0,0075	0,0304	415,978804	772,8574342
101	0,0075	0,02886	335,0623245	775,0107775

Table A.4: Data for the 10 prosumers of Power demand for every time step (t)

	Power demand (kW)									
t	Pros 1	Pros 2	Pros 3	Pros 4	Pros 5	Pros 6	Pros 7	Pros 8	Pros 9	Pros 10
1	0,1531	0,3286	0,2934	0,1474	0,0811	0,2541	0,3316	0,2022	0,7020	0,3291
2	0,1529	0,3276	0,2947	0,1474	0,0810	0,2485	0,3316	0,2022	0,6990	0,3291
3	0,1524	0,3266	0,2965	0,1471	0,0811	0,2457	0,3316	0,2022	0,6973	0,3291
4	0,1517	0,3256	0,2940	0,1469	0,0810	0,2513	0,3316	0,2022	0,5616	0,3375
5	0,1515	0,3247	0,2934	0,0808	0,0811	0,2527	0,3316	0,2022	0,5616	0,3375
6	0,1507	0,3247	0,2928	0,0807	0,0811	0,2513	0,3316	0,2022	0,5616	0,3375
7	0,1506	0,2695	0,2921	0,0807	0,0811	0,2583	0,3316	0,2022	0,5616	0,3375
8	0,1504	0,2616	0,2561	0,0805	0,0813	0,2555	0,3316	0,2022	0,5616	0,3375
9	0,1498	0,1945	0,2711	0,0808	0,0813	0,2527	0,3316	0,0890	0,5616	0,5002
10	0,1497	0,1945	0,2560	0,0805	0,0813	0,2499	0,3316	0,0890	0,5616	0,4680
11	0,1492	0,1945	0,2549	0,0808	0,0813	0,2485	0,3316	0,0890	0,5616	0,4520
12	0,1491	0,1945	0,2540	0,0807	0,0813	0,2433	0,3316	0,0890	0,6399	0,4484
13	0,1488	0,2073	0,2546	0,0806	0,0812	0,2406	0,3316	0,0890	0,6399	0,4555
14	0,1485	0,1945	0,2538	0,0810	0,0813	0,2392	0,3316	0,0890	0,6399	0,4529
15	0,1483	0,1945	0,2532	0,0810	0,0812	0,2364	1,2316	0,0890	0,6399	0,4493
16	0,1481	0,1945	0,2527	0,0810	0,0812	0,2364	1,3809	0,0890	0,6399	0,4466
17	0,1480	0,1945	0,2520	0,0810	0,0813	0,2336	1,3567	0,0890	0,6399	0,4448
18	0,1479	0,1945	0,2517	0,0810	0,0811	0,2322	0,4442	0,0890	0,6399	0,4412
19	0,1474	0,1945	0,2712	0,0808	0,0806	0,2322	0,4514	0,0805	0,6399	0,4403
20	0,1473	0,1945	0,2510	0,0809	0,0807	0,2308	0,4487	0,0805	0,6399	0,4385
21	0,1472	0,1945	0,2513	0,0808	0,1983	0,2294	0,4469	0,0805	0,6399	0,6537
22	0,0810	0,1945	0,2524	0,0808	0,2014	0,2294	0,4406	0,0805	0,6399	0,6207
23	0,0810	0,1945	0,2523	0,0810	0,1949	0,0890	0,4605	0,0805	0,6399	0,6059
24	0,0809	0,1945	0,2514	0,0807	0,1966	0,0890	0,6549	0,0805	0,6399	0,6217
25	0,0810	0,1945	0,2510	0,0808	0,1958	0,0890	0,6239	0,0805	0,6399	0,6139
26	0,0810	0,1945	0,2506	0,0808	0,1947	0,0890	0,6068	0,0805	0,6399	0,6079
27	0,0809	0,1945	0,2500	0,0809	0,1948	0,0890	0,6148	0,0805	0,6399	0,6042
28	0,0809	0,1945	0,2497	0,0808	0,1942	0,0890	0,6060	0,0805	0,7838	0,5945
29	0,0809	0,1945	0,2495	0,0809	0,1932	0,0890	0,6037	0,0805	0,7615	0,5950
30	0,0809	0,2590	0,2494	0,0807	0,1926	0,0890	0,5954	0,0805	0,7498	0,5899
31	0,0809	0,2580	0,2491	0,0806	0,2823	0,0890	0,3405	0,9805	0,7597	0,5872
32	0,0809	0,2561	0,2878	0,0808	0,2678	1,0275	0,3369	0,9805	0,7552	0,5849
33	0,3340	0,2549	0,2884	0,0810	0,2616	0,2213	0,3341	0,9805	0,7534	0,4927
34	0,2839	0,2540	0,2871	0,0809	0,2597	0,2061	0,3304	0,0805	0,7516	0,4913
35	0,2589	0,2533	0,2865	0,0806	0,2600	0,2016	0,3258	0,0805	0,7472	0,4885
36	0,2533	0,2525	0,2859	0,0807	0,2589	1,9311	0,3236	0,0805	0,7436	0,4871
37	0,2645	0,4012	0,2853	0,2214	0,2585	1,9284	0,3222	0,0805	0,7427	0,4857
38	0,2603	0,3764	0,2846	0,2002	0,2582	1,9266	0,3185	0,0805	0,7418	0,4843
39	0,2547	0,3634	0,2840	0,1909	0,2579	1,9212	0,3148	0,0805	0,7391	0,4816
40	0,2505	0,3143	0,2834	0,1900	0,2576	0,1971	0,3134	0,0805	0,7382	0,4816
41	0,2477	0,3116	0,2834	0,1909	0,2572	0,1944	0,3125	0,0805	0,6183	0,4802
42	0,2422	0,3098	0,2479	0,1900	0,2562	0,1927	0,3095	0,0805	0,6174	0,4788

Table A.5: Data for the 10 prosumers of Power demand for every time step (t)(continuation of Table A.4)

	Power demand (kW)									
t	Pros 1	Pros 2	Pros 3	Pros 4	Pros 5	Pros 6	Pros 7	Pros 8	Pros 9	Pros 10
43	0,2408	0,3036	0,4751	0,1900	0,2555	0,1909	0,3078	0,0805	0,6156	0,4710
44	0,2381	0,3036	0,3944	0,1909	0,2552	0,1891	0,3081	0,0805	0,6156	0,3306
45	0,2353	0,3009	0,3749	0,1909	0,2543	0,1873	0,2173	0,0805	0,6139	0,3306
46	0,2325	0,2991	0,3861	0,1909	0,2531	0,1864	0,2156	0,0805	0,6139	0,3306
47	0,2310	0,2973	0,3819	0,1910	0,2525	0,1855	0,0799	0,0805	0,6121	0,3306
48	0,2296	0,2955	0,3791	0,1900	0,2521	0,1837	0,0799	0,0805	0,6112	0,3306
49	0,2283	0,2938	0,3694	0,1900	0,2509	0,1837	0,0799	0,0890	0,6112	0,3306
50	0,2255	0,2929	0,3694	0,1891	0,2490	0,1828	0,0799	0,0890	0,6102	0,3306
51	0,2242	0,2929	0,3652	0,1882	0,1463	0,1735	0,0799	0,0890	0,5209	0,3306
52	0,2241	0,2911	0,3624	0,1873	0,1456	0,1717	0,0799	0,0890	0,5209	0,3306
53	0,2227	0,2902	0,3596	0,1863	0,1463	0,1717	0,0799	0,0890	0,5209	0,3306
54	0,2213	0,2902	0,3568	0,2675	0,1457	0,1717	0,0799	0,0890	0,5209	0,3306
55	0,2213	0,2893	0,3541	0,2585	0,1457	0,1699	0,0799	0,0890	0,5209	0,3306
56	0,2199	0,2875	0,3527	0,2551	0,1451	0,0805	0,0799	0,0890	0,5209	0,2893
57	0,0809	0,2866	0,3527	0,2552	0,1445	0,0805	0,0799	0,0890	0,5209	0,2893
58	0,0809	0,2860	0,3499	0,2537	0,1444	0,0805	0,0799	0,0890	0,5209	0,3383
59	0,0809	0,2851	0,3485	0,2542	0,1444	0,0805	0,0799	0,0890	0,5209	0,3383
60	0,0809	0,2842	0,3485	0,2530	0,1438	0,0805	0,0799	0,0884	0,5209	0,3383
61	0,0809	0,2842	0,3471	0,2527	0,1438	0,0805	0,0799	0,0884	0,2714	0,3383
62	0,0809	0,2833	0,3443	0,2513	0,1432	0,0805	0,0799	0,0884	0,2714	0,3299
63	0,0809	0,3458	0,3429	0,2497	0,1432	0,0805	0,0799	0,0884	0,2714	0,3299
64	0,0809	0,3451	0,3421	0,2494	0,1429	0,0805	0,0799	0,3053	0,2714	0,3299
65	0,0808	0,3428	0,3822	0,2487	0,0811	0,0805	0,0799	0,2733	0,2714	0,3299
66	0,0809	0,2543	0,3802	0,2476	0,0812	0,0805	0,0799	0,2594	0,2714	0,3299
67	0,0809	0,2532	0,3789	0,2499	0,0811	0,0805	0,0799	0,2761	0,2714	0,3299
68	0,0809	0,2525	0,3768	0,2483	0,0811	0,0805	0,0799	0,2692	0,2714	0,3299
69	0,0809	0,2520	0,3764	0,2483	0,0814	0,0805	0,0799	0,2650	0,2714	0,3299
70	0,0808	0,2512	0,3755	0,2473	0,0812	0,0805	0,0799	0,2622	0,2714	0,3299
71	0,0809	0,2510	0,3734	0,1511	0,0812	0,0805	0,0799	0,2525	0,2714	0,3299
72	0,0809	0,1939	0,2364	0,1509	0,0812	0,0805	0,0799	0,2539	0,2714	0,3299
73	0,1565	0,1939	0,2360	0,1506	0,0810	0,0805	0,0799	0,2497	0,2714	0,3299
74	0,1586	0,1939	0,2357	0,1503	0,0811	0,0805	0,0799	0,3864	0,2714	0,3299
75	0,1543	0,1939	0,1995	0,1506	0,0809	0,0805	0,0799	0,3644	0,2714	0,3299
76	0,1555	0,1939	0,1995	0,1503	0,0810	0,0805	0,0799	0,3527	0,2714	0,3299
77	0,1550	0,1939	0,1995	0,1499	0,0809	0,0805	0,0799	0,3620	0,2714	0,3299
78	0,1543	0,1939	0,1995	0,1495	0,0812	0,0805	0,0799	0,3548	0,2714	0,3299
79	0,1542	0,1939	0,1995	0,1490	0,0812	0,0805	0,0799	0,3507	0,2714	0,3299
80	0,1539	0,1939	0,1995	0,1490	0,0812	0,0805	0,0799	0,3475	0,2714	0,3299
81	0,1534	0,1939	0,1995	0,0826	0,0810	0,0805	0,0799	0,3399	0,2714	0,3299
82	0,1529	0,1939	0,1995	0,0828	0,0812	0,0805	0,0799	0,3380	0,4953	0,3299
83	0,1525	0,1939	0,1995	0,0827	0,0811	0,0805	0,0799	0,3353	0,4606	0,3299
84	0,1519	0,1939	0,1995	0,0830	0,0812	0,0805	0,0799	0,3321	0,4425	0,3299

Table A.6: Data for the 10 prosumers of Power demand for every time step (t)(continuation of Table A.5)

	Power demand (kW)									
t	Pros 1	Pros 2	Pros 3	Pros 4	Pros 5	Pros 6	Pros 7	Pros 8	Pros 9	Pros 10
85	0,1517	0,1939	0,1995	0,0831	0,0812	0,0805	0,0799	0,3299	0,4578	0,3299
86	0,1509	0,1939	0,1995	0,0829	0,0810	0,0805	0,0799	0,3281	0,4508	0,3299
87	0,1507	0,1939	0,1995	0,0829	0,0811	0,0805	0,0799	0,1867	0,3697	0,3299
88	0,1504	0,2573	0,1995	0,0831	0,0812	0,0805	0,0799	0,1849	0,3669	0,3299
89	0,1501	0,2580	0,0805	0,0829	0,0813	0,0805	0,0799	0,1840	0,3600	0,3299
90	0,1495	0,2565	0,0805	0,0831	0,0812	0,0805	0,0799	0,1831	0,3544	0,3299
91	0,1493	0,2553	0,0805	0,0829	0,0812	0,0805	0,0799	0,1822	0,3530	0,0935
92	0,1492	0,2541	0,0805	0,0829	0,0811	0,0805	0,0799	0,1805	0,3516	0,0807
93	0,1489	0,2535	0,0805	0,0828	0,0811	0,0805	0,0799	0,1805	0,3475	0,0807
94	0,1487	0,2528	0,0805	0,0829	0,0812	0,0805	0,0799	0,1796	0,3461	0,0807
95	0,1482	0,2521	0,0805	0,0831	0,0810	0,0805	0,0799	0,1787	0,3447	0,0807
96	0,1484	0,2516	0,0805	0,0831	0,0813	0,0805	0,0799	0,1787	0,3433	0,0807
97	0,1482	0,2510	0,0805	0,0830	0,0813	0,0805	0,0799	0,0884	0,3405	0,0807
98	0,1478	0,1939	0,1208	0,0829	0,0812	0,0805	0,0799	0,0884	0,3405	0,0807
99	0,1470	0,1939	0,1205	0,0828	0,0814	0,0805	0,0927	0,0884	0,3377	0,0807
100	0,1471	0,1939	0,1198	0,0830	0,2092	0,0805	0,2194	0,0884	0,3377	0,0807
101	0,1467	0,1939	0,1193	0,0828	0,1967	0,0805	0,2006	0,0884	0,3350	0,0807

Table A.7: Data for the 10 prosumers of Heat demand for every time step (t) [8]

	Heat Demand (kW)									
	Pros 1	Pros 2	Pros 3	Pros 4	Pros 5	Pros 6	Pros 7	Pros 8	Pros 9	Pros 10
1	0,1531	0,3286	0,2934	0,1474	0,0811	0,2541	0,3316	0,2022	0,7020	0,3291
2	0,1529	0,3276	0,2947	0,1474	0,0810	0,2485	0,3316	0,2022	0,6990	0,3291
3	0,1524	0,3266	0,2965	0,1471	0,0811	0,2457	0,3316	0,2022	0,6973	0,3291
4	0,1517	0,3256	0,2940	0,1469	0,0810	0,2513	0,3316	0,2022	0,5616	0,3375
5	0,1515	0,3247	0,2934	0,0808	0,0811	0,2527	0,3316	0,2022	0,5616	0,3375
6	0,1507	0,3247	0,2928	0,0807	0,0811	0,2513	0,3316	0,2022	0,5616	0,3375
7	0,1506	0,2695	0,2921	0,0807	0,0811	0,2583	0,3316	0,2022	0,5616	0,3375
8	0,1504	0,2616	0,2561	0,0805	0,0813	0,2555	0,3316	0,2022	0,5616	0,3375
9	0,1498	0,1945	0,2711	0,0808	0,0813	0,2527	0,3316	0,0890	0,5616	0,5002
10	0,1497	0,1945	0,2560	0,0805	0,0813	0,2499	0,3316	0,0890	0,5616	0,4680
11	0,1492	0,1945	0,2549	0,0808	0,0813	0,2485	0,3316	0,0890	0,5616	0,4520
12	0,1491	0,1945	0,2540	0,0807	0,0813	0,2433	0,3316	0,0890	0,6399	0,4484
13	0,1488	0,2073	0,2546	0,0806	0,0812	0,2406	0,3316	0,0890	0,6399	0,4555
14	0,1485	0,1945	0,2538	0,0810	0,0813	0,2392	0,3316	0,0890	0,6399	0,4529
15	0,1483	0,1945	0,2532	0,0810	0,0812	0,2364	1,2316	0,0890	0,6399	0,4493
16	0,1481	0,1945	0,2527	0,0810	0,0812	0,2364	1,3809	0,0890	0,6399	0,4466
17	0,1480	0,1945	0,2520	0,0810	0,0813	0,2336	1,3567	0,0890	0,6399	0,4448
18	0,1479	0,1945	0,2517	0,0810	0,0811	0,2322	0,4442	0,0890	0,6399	0,4412
19	0,1474	0,1945	0,2712	0,0808	0,0806	0,2322	0,4514	0,0805	0,6399	0,4403
20	0,1473	0,1945	0,2510	0,0809	0,0807	0,2308	0,4487	0,0805	0,6399	0,4385
21	0,1472	0,1945	0,2513	0,0808	0,1983	0,2294	0,4469	0,0805	0,6399	0,6537
22	0,0810	0,1945	0,2524	0,0808	0,2014	0,2294	0,4406	0,0805	0,6399	0,6207
23	0,0810	0,1945	0,2523	0,0810	0,1949	0,0890	0,4605	0,0805	0,6399	0,6059
24	0,0809	0,1945	0,2514	0,0807	0,1966	0,0890	0,6549	0,0805	0,6399	0,6217
25	0,0810	0,1945	0,2510	0,0808	0,1958	0,0890	0,6239	0,0805	0,6399	0,6139
26	0,0810	0,1945	0,2506	0,0808	0,1947	0,0890	0,6068	0,0805	0,6399	0,6079
27	0,0809	0,1945	0,2500	0,0809	0,1948	0,0890	0,6148	0,0805	0,6399	0,6042
28	0,0809	0,1945	0,2497	0,0808	0,1942	0,0890	0,6060	0,0805	0,7838	0,5945
29	0,0809	0,1945	0,2495	0,0809	0,1932	0,0890	0,6037	0,0805	0,7615	0,5950
30	0,0809	0,2590	0,2494	0,0807	0,1926	0,0890	0,5954	0,0805	0,7498	0,5899
31	0,0809	0,2580	0,2491	0,0806	0,2823	0,0890	0,3405	0,9805	0,7597	0,5872
32	0,0809	0,2561	0,2878	0,0808	0,2678	1,0275	0,3369	0,9805	0,7552	0,5849
33	0,3340	0,2549	0,2884	0,0810	0,2616	0,2213	0,3341	0,9805	0,7534	0,4927
34	0,2839	0,2540	0,2871	0,0809	0,2597	0,2061	0,3304	0,0805	0,7516	0,4913
35	0,2589	0,2533	0,2865	0,0806	0,2600	0,2016	0,3258	0,0805	0,7472	0,4885
36	0,2533	0,2525	0,2859	0,0807	0,2589	1,9311	0,3236	0,0805	0,7436	0,4871
37	0,2645	0,4012	0,2853	0,2214	0,2585	1,9284	0,3222	0,0805	0,7427	0,4857
38	0,2603	0,3764	0,2846	0,2002	0,2582	1,9266	0,3185	0,0805	0,7418	0,4843
39	0,2547	0,3634	0,2840	0,1909	0,2579	1,9212	0,3148	0,0805	0,7391	0,4816
40	0,2505	0,3143	0,2834	0,1900	0,2576	0,1971	0,3134	0,0805	0,7382	0,4816
41	0,2477	0,3116	0,2834	0,1909	0,2572	0,1944	0,3125	0,0805	0,6183	0,4802
42	0,2422	0,3098	0,2479	0,1900	0,2562	0,1927	0,3095	0,0805	0,6174	0,4788

Table A.8: Data for the 10 prosumers of Heat demand for every time step (t) [8] (continuation of Table A.7)

	Heat Demand (kW)									
	Pros 1	Pros 2	Pros 3	Pros 4	Pros 5	Pros 6	Pros 7	Pros 8	Pros 9	Pros 10
43	0,2408	0,3036	0,4751	0,1900	0,2555	0,1909	0,3078	0,0805	0,6156	0,4710
44	0,2381	0,3036	0,3944	0,1909	0,2552	0,1891	0,3081	0,0805	0,6156	0,3306
45	0,2353	0,3009	0,3749	0,1909	0,2543	0,1873	0,2173	0,0805	0,6139	0,3306
46	0,2325	0,2991	0,3861	0,1909	0,2531	0,1864	0,2156	0,0805	0,6139	0,3306
47	0,2310	0,2973	0,3819	0,1910	0,2525	0,1855	0,0799	0,0805	0,6121	0,3306
48	0,2296	0,2955	0,3791	0,1900	0,2521	0,1837	0,0799	0,0805	0,6112	0,3306
49	0,2283	0,2938	0,3694	0,1900	0,2509	0,1837	0,0799	0,0890	0,6112	0,3306
50	0,2255	0,2929	0,3694	0,1891	0,2490	0,1828	0,0799	0,0890	0,6102	0,3306
51	0,2242	0,2929	0,3652	0,1882	0,1463	0,1735	0,0799	0,0890	0,5209	0,3306
52	0,2241	0,2911	0,3624	0,1873	0,1456	0,1717	0,0799	0,0890	0,5209	0,3306
53	0,2227	0,2902	0,3596	0,1863	0,1463	0,1717	0,0799	0,0890	0,5209	0,3306
54	0,2213	0,2902	0,3568	0,2675	0,1457	0,1717	0,0799	0,0890	0,5209	0,3306
55	0,2213	0,2893	0,3541	0,2585	0,1457	0,1699	0,0799	0,0890	0,5209	0,3306
56	0,2199	0,2875	0,3527	0,2551	0,1451	0,0805	0,0799	0,0890	0,5209	0,2893
57	0,0809	0,2866	0,3527	0,2552	0,1445	0,0805	0,0799	0,0890	0,5209	0,2893
58	0,0809	0,2860	0,3499	0,2537	0,1444	0,0805	0,0799	0,0890	0,5209	0,3383
59	0,0809	0,2851	0,3485	0,2542	0,1444	0,0805	0,0799	0,0890	0,5209	0,3383
60	0,0809	0,2842	0,3485	0,2530	0,1438	0,0805	0,0799	0,0884	0,5209	0,3383
61	0,0809	0,2842	0,3471	0,2527	0,1438	0,0805	0,0799	0,0884	0,2714	0,3383
62	0,0809	0,2833	0,3443	0,2513	0,1432	0,0805	0,0799	0,0884	0,2714	0,3299
63	0,0809	0,3458	0,3429	0,2497	0,1432	0,0805	0,0799	0,0884	0,2714	0,3299
64	0,0809	0,3451	0,3421	0,2494	0,1429	0,0805	0,0799	0,3053	0,2714	0,3299
65	0,0808	0,3428	0,3822	0,2487	0,0811	0,0805	0,0799	0,2733	0,2714	0,3299
66	0,0809	0,2543	0,3802	0,2476	0,0812	0,0805	0,0799	0,2594	0,2714	0,3299
67	0,0809	0,2532	0,3789	0,2499	0,0811	0,0805	0,0799	0,2761	0,2714	0,3299
68	0,0809	0,2525	0,3768	0,2483	0,0811	0,0805	0,0799	0,2692	0,2714	0,3299
69	0,0809	0,2520	0,3764	0,2483	0,0814	0,0805	0,0799	0,2650	0,2714	0,3299
70	0,0808	0,2512	0,3755	0,2473	0,0812	0,0805	0,0799	0,2622	0,2714	0,3299
71	0,0809	0,2510	0,3734	0,1511	0,0812	0,0805	0,0799	0,2525	0,2714	0,3299
72	0,0809	0,1939	0,2364	0,1509	0,0812	0,0805	0,0799	0,2539	0,2714	0,3299
73	0,1565	0,1939	0,2360	0,1506	0,0810	0,0805	0,0799	0,2497	0,2714	0,3299
74	0,1586	0,1939	0,2357	0,1503	0,0811	0,0805	0,0799	0,3864	0,2714	0,3299
75	0,1543	0,1939	0,1995	0,1506	0,0809	0,0805	0,0799	0,3644	0,2714	0,3299
76	0,1555	0,1939	0,1995	0,1503	0,0810	0,0805	0,0799	0,3527	0,2714	0,3299
77	0,1550	0,1939	0,1995	0,1499	0,0809	0,0805	0,0799	0,3620	0,2714	0,3299
78	0,1543	0,1939	0,1995	0,1495	0,0812	0,0805	0,0799	0,3548	0,2714	0,3299
79	0,1542	0,1939	0,1995	0,1490	0,0812	0,0805	0,0799	0,3507	0,2714	0,3299
80	0,1539	0,1939	0,1995	0,1490	0,0812	0,0805	0,0799	0,3475	0,2714	0,3299
81	0,1534	0,1939	0,1995	0,0826	0,0810	0,0805	0,0799	0,3399	0,2714	0,3299
82	0,1529	0,1939	0,1995	0,0828	0,0812	0,0805	0,0799	0,3380	0,4953	0,3299
83	0,1525	0,1939	0,1995	0,0827	0,0811	0,0805	0,0799	0,3353	0,4606	0,3299
84	0,1519	0,1939	0,1995	0,0830	0,0812	0,0805	0,0799	0,3321	0,4425	0,3299

Table A.9: Data for the 10 prosumers of Heat demand for every time step (t) [8] (continuation of Table A.8)

	Heat Demand (kW)									
	Pros 1	Pros 2	Pros 3	Pros 4	Pros 5	Pros 6	Pros 7	Pros 8	Pros 9	Pros 10
85	0,1517	0,1939	0,1995	0,0831	0,0812	0,0805	0,0799	0,3299	0,4578	0,3299
86	0,1509	0,1939	0,1995	0,0829	0,0810	0,0805	0,0799	0,3281	0,4508	0,3299
87	0,1507	0,1939	0,1995	0,0829	0,0811	0,0805	0,0799	0,1867	0,3697	0,3299
88	0,1504	0,2573	0,1995	0,0831	0,0812	0,0805	0,0799	0,1849	0,3669	0,3299
89	0,1501	0,2580	0,0805	0,0829	0,0813	0,0805	0,0799	0,1840	0,3600	0,3299
90	0,1495	0,2565	0,0805	0,0831	0,0812	0,0805	0,0799	0,1831	0,3544	0,3299
91	0,1493	0,2553	0,0805	0,0829	0,0812	0,0805	0,0799	0,1822	0,3530	0,0935
92	0,1492	0,2541	0,0805	0,0829	0,0811	0,0805	0,0799	0,1805	0,3516	0,0807
93	0,1489	0,2535	0,0805	0,0828	0,0811	0,0805	0,0799	0,1805	0,3475	0,0807
94	0,1487	0,2528	0,0805	0,0829	0,0812	0,0805	0,0799	0,1796	0,3461	0,0807
95	0,1482	0,2521	0,0805	0,0831	0,0810	0,0805	0,0799	0,1787	0,3447	0,0807
96	0,1484	0,2516	0,0805	0,0831	0,0813	0,0805	0,0799	0,1787	0,3433	0,0807
97	0,1482	0,2510	0,0805	0,0830	0,0813	0,0805	0,0799	0,0884	0,3405	0,0807
98	0,1478	0,1939	0,1208	0,0829	0,0812	0,0805	0,0799	0,0884	0,3405	0,0807
99	0,1470	0,1939	0,1205	0,0828	0,0814	0,0805	0,0927	0,0884	0,3377	0,0807
100	0,1471	0,1939	0,1198	0,0830	0,2092	0,0805	0,2194	0,0884	0,3377	0,0807
101	0,1467	0,1939	0,1193	0,0828	0,1967	0,0805	0,2006	0,0884	0,3350	0,0807